

# Methods for approximating stochastic evolutionary dynamics on graphs

Christopher E. Overton<sup>a,\*</sup>, Mark Broom<sup>b</sup>, Christoforos Hadjichrysanthou<sup>c</sup>, Kieran J. Sharkey<sup>a</sup>

<sup>a</sup>*Department of Mathematical Sciences, University of Liverpool, Mathematical Sciences Building, Liverpool L69 7ZL, UK.*

<sup>b</sup>*Department of Mathematics, City, University of London, Northampton Square, London EC1V 0HB, UK.*

<sup>c</sup>*Department of Infectious Disease Epidemiology, School of Public Health, Imperial College London, St Mary's Campus, Norfolk Place, London W2 1PG, UK.*

---

## Abstract

Population structure can have a significant effect on evolution. For some systems with sufficient symmetry, analytic results can be derived within the mathematical framework of evolutionary graph theory which relate to the outcome of the evolutionary process. However, for more complicated heterogeneous structures, computationally intensive methods are required such as individual-based stochastic simulations. By adapting methods from statistical physics, including moment closure techniques, we first show how to derive existing homogenised pair approximation models and the exact neutral drift model. We then develop node-level approximations to stochastic evolutionary processes on arbitrarily complex structured populations represented by finite graphs, which can capture the different dynamics for individual nodes in the population. Using these approximations, we evaluate the fixation probability of invading mutants for given initial conditions, where the dynamics follow standard evolutionary processes such as the invasion process. Comparisons with the output of stochastic simulations reveal the effectiveness of our approximations in describing the stochastic processes and in predicting the probability of fixation of mutants on a wide range of graphs. Construction of these models facilitates a systematic analysis and is valuable for a greater understanding of the influence of population structure on evolutionary processes.

*Keywords:* evolutionary graph theory, moment closure, fixation probability, network, Markov process

---

## 1. Introduction

1 Models of evolutionary dynamics were originally deterministic and assumed well-mixed populations in  
2 which every individual of a given type is identical. Stochastic models of these finite well-mixed popula-  
3 tions [25] have been studied, however real populations are usually characterised by a complicated relationship  
4 structure between individuals [42]. To account for this, a class of mathematical models known as evolutionary  
5 graph theory have been developed which show that the population structure can significantly influence the  
6 outcome of evolutionary dynamics [20, 40]. In these models, structured populations are represented by finite  
7 graphs, where each node represents an individual in the population and relationships between individuals  
8 are represented by the edges of the graph. Stochastic evolutionary processes can be considered analytically  
9 and precise results can be derived for a number of simple graphs, such as the circle, star and complete  
10 graphs [5, 6, 20], mainly due to their symmetry. Analytic approaches for investigating evolutionary dynam-  
11 ics on complex graphs have also been proposed. However, such methods are usually limited by assumptions  
12 such as large populations [27, 28] or are specifically designed for investigating evolutionary processes under  
13 weak selection [1, 43], where the evolutionary game has only a small effect on reproductive success.

14 Important quantities of interest such as the exact fixation probability and time can, in principle, be  
15 obtained by solving the discrete-time difference equations of the underlying stochastic model [11], although  
16 this is only feasible for very small populations unless there are simplifying symmetries. Individual-based  
17 stochastic simulations [3, 21] provide numerically accurate representations of the evolutionary process on  
18 arbitrary graphs but have limited scope for generating conceptual insights into the dynamics on their own.

---

\*Corresponding author

*Email address:* C.Overton@liverpool.ac.uk (Christopher E. Overton)

19 They can also be computationally expensive on larger graphs, but as a precise representation of the underlying  
20 stochastic model, they allow us to evaluate the accuracy of approximate models by comparison.

21 Here we develop approximations to the stochastic model by using insights from methods in statistical  
22 physics that have also been used extensively for epidemic modelling [4, 14, 16, 29, 33, 34]. Such methods  
23 have been applied to develop pair approximations for evolutionary processes on graphs which satisfy the  
24 homogeneity assumption that all individuals can be considered identical and interchangeable [8, 10, 26, 30, 37].  
25 However, the underlying assumptions linking these models to the underlying stochastic dynamics are not  
26 always clear. One contribution of this work is to derive these models explicitly by identifying the required  
27 assumptions. The starting point for all of our approximations is to derive an equation to describe the time-  
28 evolution of the state of any given individual node. From this equation, various routes to approximation  
29 become apparent by applying different assumptions. We then investigate the applicability and accuracy of  
30 the resulting approximation methods.

31 Evolutionary graph theory is traditionally explored as a discrete-time stochastic model. While it is  
32 possible to work with these dynamics, it is easier to work with a continuous-time approximation to the  
33 process. The continuous-time system is represented by a master equation describing how the probability of  
34 being in each system state changes. From the master equation we obtain exact equations (with respect to  
35 the continuous-time process) for the probabilities of the states of individual nodes (Theorem 2.1). These  
36 equations can then be approximated by adopting moment-closure methods. We focus on evaluating the  
37 probability that at the end of the evolutionary process, an initial subset of mutants placed on the graph  
38 will take over the whole population and ‘fixate’. Using this continuous-time system is justified because the  
39 fixation probability and expected time to fixation are identical to those of the original discrete-time process.  
40 Within this framework we study when accurate approximations can be derived.

41 In Sections 2.1-2.3 we introduce the stochastic evolutionary dynamics and the master equation, and  
42 derive a description of how node-level quantities change in the master equation. We then discuss and  
43 develop various techniques that can be used to approximate these systems of equations in Section 3. Within  
44 these approximation frameworks we derive the pair approximation models used in the literature, which we  
45 will call the homogenised pair approximation, and the exact neutral drift model, and build new node level  
46 approximation methods. In Section 4 we demonstrate how the different methods can be used to approximate  
47 the dynamics of the original discrete-time process. Section 4.1 studies how the methods perform when  
48 approximating the fixation probability of a single initial mutant placed on idealised and on complex graphs.  
49 Section 4.2 then shows how the methods perform when studying the evolutionary game dynamics in a Hawk-  
50 Dove game. In Section 5 we discuss the results obtained from the methods developed and the insights these  
51 can give.

## 52 2. The stochastic model

### 53 2.1. Stochastic evolutionary dynamics

54 We consider a population whose relationship structure is represented by a strongly connected undirected  
55 graph  $(V, E)$  where  $V = \{1, 2, \dots, N\}$  is the set of nodes and  $E$  denotes the set of edges. This can be  
56 represented by an adjacency matrix  $G$ , where  $G_{ij} = 1$  if  $j$  is connected to  $i$ , and  $G_{ij} = 0$  otherwise, with  
57  $G_{ii} = 0$  for all  $i \in V$ . We consider populations consisting of two types of individuals, type  $A$  and type  
58  $B$ , either of which can be in the role of invading mutant in a resident population. Each node is occupied  
59 by either an  $A$  or a  $B$  individual. Therefore we can let  $A_i = 1$  if and only if node  $i$  is occupied by an  $A$   
60 individual and  $A_i = 0$  otherwise and let  $B_i$  denote the same for individuals of type  $B$ . Since  $B_i = 1 - A_i$ ,  
61 the state of the system can be represented by the values of  $A_i$  at any given time. If there exists an edge  
62  $(i, j) \in E$  between nodes  $i, j \in V$ , then the offspring of the individual in node  $j$  can replace the individual in  
63 node  $i$  and vice versa. To study the evolutionary dynamics between these two types of individual we require  
64 a measure of fitness. We can describe the fitness payoff received from interactions between individuals by  
65 the following payoff matrix:

$$\begin{array}{cc} & \begin{array}{cc} A & B \end{array} \\ \begin{array}{c} A \\ B \end{array} & \begin{pmatrix} a & b \\ c & d \end{pmatrix}, \end{array}$$

66 where an  $A$  individual obtains a payoff  $a$  when interacting with another  $A$  individual and payoff  $b$  when  
 67 interacting with a  $B$  individual. Similarly, a  $B$  individual obtains payoffs  $c$  and  $d$  when interacting with an  
 68  $A$  individual and a  $B$  individual respectively.

69 To define fitness based on the payoff, following similar definitions in the literature [9, 20, 28, 40, 38],  
 70 the fitness of each individual is assumed to be  $f = f_{back} + wP$ , where  $f_{back}$  is the background fitness of all  
 71 individuals,  $P$  is the average payoff received from interactions with neighbours, and  $w \in [0, \infty)$  is a parameter  
 72 which controls the contribution of the game payoff to fitness.

73 The fitness of an  $A$  individual which occupies node  $j$ ,  $f_A^j$ , is therefore given by

$$f_A^j = f_{back} + w \frac{a \sum_{i=1}^N G_{ij} A_i + b \sum_{i=1}^N G_{ij} B_i}{\sum_{i=1}^N G_{ij}}, \quad (1)$$

74 and similarly the fitness of a  $B$  individual occupying node  $j$  is given by

$$f_B^j = f_{back} + w \frac{c \sum_{i=1}^N G_{ij} A_i + d \sum_{i=1}^N G_{ij} B_i}{\sum_{i=1}^N G_{ij}}. \quad (2)$$

75 In the special case of constant fitness, where the fitness of individuals remains constant independent of the  
 76 interactions with other individuals, we take the payoff matrix as

$$\begin{array}{cc} & \begin{array}{cc} A & B \end{array} \\ \begin{array}{c} A \\ B \end{array} & \begin{pmatrix} r & r \\ 1 & 1 \end{pmatrix}, \end{array}$$

77 so that  $A$  individuals have relative payoff equal to  $r$ .

78 Traditional evolutionary graph theory considers a discrete-time Markovian evolutionary process in which  
 79 only one event can happen at each time step. When an event occurs, one individual reproduces and a  
 80 connected individual dies, with the offspring replacing it. We refer to the mechanism by which this takes  
 81 place as an update mechanism or rule. The probability of a certain event taking place depends upon  
 82 this update mechanism. Some of the most commonly considered update mechanisms are birth-death with  
 83 selection on birth (invasion process) [20], death-birth with selection on birth [22], birth-death with selection  
 84 on death [2] and death-birth with selection on death (voter model) [28]. The methods developed in this  
 85 paper will be presented in the general case, and can be applied to any of the above update rules, but we  
 86 shall focus on the invasion process when generating specific examples. In the invasion process, we select an  
 87 individual to reproduce in proportion to their fitness (selection on birth) and then the offspring replaces a  
 88 connected individual selected uniformly at random for death (birth then death).

## 89 2.2. The master equation

90 To approximate the discrete-time evolutionary process we first translate the discrete-time system to an  
 91 approximate continuous-time system. To do this we model each (replacement) event using a Poisson process.  
 92 The rate at which each event happens is equal to the probability of that event in the discrete-time model.  
 93 Therefore the total event pressure will be the sum of all such probabilities, which is equal to one, so that  
 94 the time until the next event follows a Poisson process with rate parameter one. We then determine which  
 95 event takes place using the relevant probability. Under this continuous-time system the fixation probability  
 96 and expected time to fixation will be identical to those of the discrete-time system, since we use the same  
 97 probabilities whenever an event occurs and the expected time between events is constant. This is important  
 98 because these are the main quantities of interest in evolutionary dynamics.

99 We will use this system to build approximation methods to study the original discrete-time process. We  
 100 choose to use continuous-time because it enables us to build a system of ordinary differential equations to

101 approximate the dynamics, which allow us to make use of efficient numerical solvers and enable us to derive  
 102 some analytic results.

103 Since this evolutionary process is a continuous-time Markov process, we can construct a master equation  
 104 to describe the dynamics. Let  $S_i = (s_1, s_2, \dots, s_N)$  be a state of the system, where  $i \in \{1, \dots, 2^N\}$  and where  
 105  $s_j = 1$  if node  $j$  is a type  $A$  individual and  $s_j = 0$  otherwise. We define  $S_1 = (0, 0, \dots, 0)$  and  $S_{2^N} = (1, 1, \dots, 1)$   
 106 to be the states consisting of only  $B$  individuals and only  $A$  individuals, respectively.

107 We introduce a vector  $\mathbf{p}(t)$  which represents the probabilities of each system state at time  $t$ . That is,  
 108 the  $i$ th entry of  $\mathbf{p}(t)$ ,  $p_i(t)$ , is the probability that the system is in state  $S_i$  at time  $t$ . This Markovian  
 109 evolutionary process has  $2^N$  possible states and the transitions between them are governed by a  $2^N \times 2^N$   
 110 transition rate matrix  $R$  whose entries depend upon the graph and update mechanism we consider.

111 We write the rate of change in the state probabilities using the master equation of the Markov process:

$$\frac{d\mathbf{p}}{dt} = R\mathbf{p}. \quad (3)$$

112 Such an equation can be constructed for any graph under a Markovian update mechanism. The absorbing  
 113 states correspond to the all type  $B$  or all type  $A$  states,  $S_1$  and  $S_{2^N}$ , so are given by  $p_1$  and  $p_{2^N}$ .

114 Since we consider a strongly connected adjacency matrix  $G$ , provided we have at least one type  $A$  and one  
 115 type  $B$  it is possible to get to either of the absorbing states and therefore from any mixed initial condition the  
 116 system will always end up distributed between these two states. We define the fixation probability  $P_{fix}^A(S(i))$   
 117 of type  $A$  from an initial state  $S(i)$  to be the probability of being in the all  $A$  absorbing state, that is

$$P_{fix}^A(S_i) = \lim_{t \rightarrow \infty} (p_{2^N}(t) | p_i(0) = 1),$$

118 where  $p_i(0)$  is the probability of being in the state  $S_i$  at time  $t = 0$ . Similarly we define the fixation  
 119 probability of type  $B$  as

$$P_{fix}^B(S_i) = \lim_{t \rightarrow \infty} (p_1(t) | p_i(0) = 1).$$

120 The computational cost of implementing system (3) increases exponentially with  $N$  [11], and thus the  
 121 computation of the fixation probability becomes infeasible as the population size increases. Therefore it  
 122 is of interest to build approximation methods. Pair approximations of the master equation have been  
 123 developed under the homogeneity assumption that all nodes on the underlying graph are identical and  
 124 interchangeable [10, 37], which can give interesting insight into the evolutionary dynamics. However the  
 125 homogeneity assumptions made in these approximations result in the loss of insight into graph and node-  
 126 specific dynamics, so we aim to develop approximations of the master equation which can capture this  
 127 information.

### 128 2.3. Node level equations

129 We approximate the master equation by approximating the dynamics of the state probabilities of in-  
 130 dividual nodes in the population. This is motivated by approaches in statistical physics and epidemic  
 131 modelling [4, 16, 33, 34], and first requires exact equations describing how the probability of each node being  
 132 occupied by a certain type changes with time, which can be derived from the master equation (3).

133 **Definition 2.1.** Let  $\chi(\Omega_{j \rightarrow i}^t | S^t)$  denote the rate at which the individual in node  $j$  replaces the individual  
 134 in node  $i$  at time  $t$  given that the system is in state  $S$  at time  $t$ ; we refer to this as the replacement rate.

135 **Definition 2.2.**  $X_C^t$  denotes the event that the set of nodes  $C$  is in state  $X$  at time  $t$ ; for example  $A_{\{i\}}^t$  is  
 136 the event that node  $i$  is in the type  $A$  state at time  $t$ .

137 Throughout this paper we shall use the shorthand  $B_{\{i\}}^t A_{\{j\}}^t X_C^t$  to represent the intersection of events  
 138  $B_{\{i\}}^t \cap A_{\{j\}}^t \cap X_C^t$ .

139 **Theorem 2.1.** Under any Markovian update mechanism, for a structured population represented by the  
 140 adjacency matrix  $G$ , the rate of change of the probability that the individual in node  $i$  is an  $A$  individual is

$$\begin{aligned} \frac{dP(A_{\{i\}}^t)}{dt} &= \sum_{j=1}^N \sum_{X_{V \setminus \{i,j\}}} G_{ij} P(B_{\{i\}}^t A_{\{j\}}^t X_{V \setminus \{i,j\}}^t) \chi(\Omega_{j \rightarrow i}^t | B_{\{i\}}^t A_{\{j\}}^t X_{V \setminus \{i,j\}}^t) \\ &\quad - \sum_{j=1}^N \sum_{X_{V \setminus \{i,j\}}} G_{ij} P(A_{\{i\}}^t B_{\{j\}}^t X_{V \setminus \{i,j\}}^t) \chi(\Omega_{j \rightarrow i}^t | A_{\{i\}}^t B_{\{j\}}^t X_{V \setminus \{i,j\}}^t), \end{aligned} \quad (4)$$

141 where the sum over  $X_{V \setminus \{i,j\}}$  is over all possible states of the nodes  $V \setminus \{i,j\}$ .

142 *Proof.* See Appendix A.

143 This theorem can be applied to any update mechanism by choosing an appropriate definition for the  
144 replacement rate,  $\chi(\Omega_{j \rightarrow i}^t)$ , which we shall define for the invasion process as an example.

145 **Example 2.1** (Invasion process). *The invasion process is an adaptation of the Moran process [25] to struc-*  
146 *tured populations. Each event is determined by selecting an individual to reproduce with probability propor-*  
147 *tional to its fitness. It produces an identical offspring which replaces one of the connected individuals which*  
148 *is chosen uniformly at random. Therefore the rate at which the individual in node  $j$  replaces the individual*  
149 *in node  $i$  at time  $t$  under the invasion process rules is given by*

$$\chi(\Omega_{j \rightarrow i}^t | S) = \frac{f_j^t | S}{F^t | S} \frac{1}{k_j}, \quad (5)$$

150 where  $f_j^t$  is the fitness of the individual occupying node  $j$  at time  $t$ ,  $F^t = \sum_{m=1}^N f_m^t$  is the total fitness of the  
151 population, and  $k_j$  denotes the degree of node  $j$ . Here, the factor  $f_j^t / F^t$  is the rate at which node  $j$  is selected  
152 to reproduce, and  $1/k_j$  is the probability of replacing the neighbouring individual  $i$  which is selected uniformly  
153 at random.

154 When calculating  $\chi(\Omega_{j \rightarrow i}^t)$  in Equation (4), we will use the following expression for the fitness of the  
155 individual at a given node  $j$  at time  $t$ ,

$$f_j^t = f_{back} + w P(A_{\{j\}}^t) \frac{a \sum_{i=1}^N G_{ij} P(A_{\{i\}}^t) + b \sum_{i=1}^N G_{ij} P(B_{\{i\}}^t)}{\sum_{i=1}^N G_{ij}} + w P(B_{\{j\}}^t) \frac{c \sum_{i=1}^N G_{ij} P(A_{\{i\}}^t) + d \sum_{i=1}^N G_{ij} P(B_{\{i\}}^t)}{\sum_{i=1}^N G_{ij}}, \quad (6)$$

156 which is a sum of equations (1) and (2) weighted by the node probabilities. We use this definition because  
157 when we evaluate Equation (6) given that the system is in a particular state  $S$ , as required by Equation (4),  
158 the values of  $P(A_{\{k\}}^t)$  and  $P(B_{\{k\}}^t)$  are either 1 or 0, which leads to the fitness of node  $j$  in that particular  
159 system state (Equations (1) and (2)). However, by defining fitness in terms of the node probabilities, this  
160 allows us to have a description of fitness which we can approximate (see Sections 3.2 and 3.3).

### 161 3. Approximating the stochastic model

162 In other fields, such as epidemiology, the construction of node-level equations such as Equation (4) can  
163 lead to a hierarchy of moment equations whereby these equations are written in terms of pair probabilities,  
164 pairs are written in terms of triples and so on, until the full system state size is reached and the hierarchy  
165 is closed. This is useful when we can find appropriate closure approximations to close this hierarchy at a  
166 low order. However, we see that such an approach cannot be used here because we condition against the  
167 full system state in Equation (4) which means that the full system size appears even at the first order. We  
168 therefore attempt to find other methods to simplify this system of equations.

169 In this section we will describe three different techniques to derive approximations for this system. The  
170 first technique yields a system of equations which become computationally infeasible in some circumstances,

171 but by applying homogeneity assumptions to the underlying graph, we can derive the existing pair approx-  
172 imation models currently used in the literature [8, 10, 26, 30, 37] (Section 3.1). To reduce computation  
173 costs, we then develop methods based on restricting the number of states which we condition against in  
174 the replacement rate. We first obtain a method whose computational complexity scales linearly with the  
175 population size  $N$  and, after an appropriate scaling, approximates the fixation probability well on a wide  
176 range of graphs (Section 3.2). Then, in Section 3.3, we obtain a method which, although it scales with  $N^2$ ,  
177 provides a good approximation to the evolutionary dynamics over the whole time series for various graphs,  
178 and in particular provides a very accurate approximation to the initial dynamics of the evolutionary process  
179 on all graphs.

### 180 3.1. Deriving the homogenised pair approximation model

181 One way of simplifying (4) is to assume that the fitness  $f_j^t$  does not need to be normalised by the total  
182 fitness  $F^t$  in the replacement rate (e.g. as in Equation (5) for the invasion process). This approximation  
183 is justified because it does not change the final value to which the exact node-level equations converge  
184 (and therefore the fixation probability), and will only transform the time series until fixation. Making this  
185 assumption, the node level equations simplify so that we only sum over the neighbours of the individual  
186 that we selected based on fitness. That is, when looking at the event where node  $j$  replaces node  $i$ , if we  
187 are selecting on death we need to condition against the state of all neighbours of  $i$ , and if selecting on birth  
188 we need to condition against the state of all neighbours of  $j$ . As an example, we shall assume here that  
189 selection occurs on birth so that we require conditioning on the neighbourhood of node  $j$ , however we can  
190 also make similar arguments when selecting on death. Using  $\bar{\chi}$  to represent this modification of  $\chi$  in (4) and  
191  $Q$  to represent the new probability distribution with the modified time series we obtain

$$\begin{aligned} \frac{dQ(A_{\{i\}}^t)}{dt} &= \sum_{j=1}^N \sum_{X_{\mathcal{N}_j \setminus \{i\}}} G_{ij} Q(B_{\{i\}}^t A_{\{j\}}^t X_{\mathcal{N}_j \setminus \{i\}}^t) \bar{\chi}(\Omega_{j \rightarrow i}^t | B_{\{i\}}^t A_{\{j\}}^t X_{\mathcal{N}_j \setminus \{i\}}^t) \\ &\quad - \sum_{j=1}^N \sum_{X_{\mathcal{N}_j \setminus \{i\}}} G_{ij} Q(A_{\{i\}}^t B_{\{j\}}^t X_{\mathcal{N}_j \setminus \{i\}}^t) \bar{\chi}(\Omega_{j \rightarrow i}^t | A_{\{i\}}^t B_{\{j\}}^t X_{\mathcal{N}_j \setminus \{i\}}^t), \end{aligned} \quad (7)$$

192 where  $\mathcal{N}_j$  is the neighbourhood of node  $j$ , i.e. all nodes that are connected to  $j$ . To solve this system  
193 exactly requires the development of equations describing how the probability of each possible neighbourhood  
194 of nodes changes. This in turn would lead to a hierarchy of equations which is computationally similar to  
195 the master equation. However it is possible to develop approximation methods by assuming independence at  
196 the level of lower-order terms, such as individuals or pairs of nodes, and approximating the neighbourhood  
197 probabilities as a function of these.

198 For example, we can make a pair approximation by applying Bayes' Theorem and assuming statistical  
199 independence at the level of pairs to rewrite the neighbourhood probability in terms of pair probabilities.  
200 Applying Bayes' Theorem to the probabilities on the right hand side of Equation (7) we get

$$\begin{aligned} \frac{dQ(A_{\{i\}}^t)}{dt} &= \sum_{j=1}^N \sum_{X_{\mathcal{N}_j \setminus \{i\}}} G_{ij} Q(A_{\{j\}}^t) Q(B_{\{i\}}^t X_{\mathcal{N}_j \setminus \{i\}}^t | A_{\{j\}}^t) \bar{\chi}(\Omega_{j \rightarrow i}^t | B_{\{i\}}^t A_{\{j\}}^t X_{\mathcal{N}_j \setminus \{i\}}^t) \\ &\quad - \sum_{j=1}^N \sum_{X_{\mathcal{N}_j \setminus \{i\}}} G_{ij} Q(B_{\{j\}}^t) Q(A_{\{i\}}^t X_{\mathcal{N}_j \setminus \{i\}}^t | B_{\{j\}}^t) \bar{\chi}(\Omega_{j \rightarrow i}^t | A_{\{i\}}^t B_{\{j\}}^t X_{\mathcal{N}_j \setminus \{i\}}^t). \end{aligned} \quad (8)$$

201 If we assume statistical independence of all nodes in the neighbourhood of  $j$ , given the state of  $j$ , we can  
202 rewrite the neighbourhood probability  $Q(A_{\{j\}}^t) Q(B_{\{i\}}^t X_{\mathcal{N}_j \setminus \{i\}}^t | A_{\{j\}}^t)$  as

$$Q(A_{\{j\}}^t) Q(B_{\{i\}}^t X_{\mathcal{N}_j \setminus \{i\}}^t | A_{\{j\}}^t) \approx Q(A_{\{j\}}^t) Q(B_{\{i\}}^t | A_{\{j\}}^t) \prod_{l \in \mathcal{N}_j \setminus \{i\}} Q(X_{\{l\}}^t | A_{\{j\}}^t),$$

203 where  $X_{\{l\}}^t$  is event where node  $l$  is in the same state as it is in the event  $X_{\mathcal{N}_j \setminus \{i\}}^t$ . Substituting this into  
 204 Equation (8) gives

$$\begin{aligned} \frac{dQ(A_{\{i\}}^t)}{dt} &\approx \sum_{j=1}^N \sum_{X_{\mathcal{N}_j \setminus \{i\}}} G_{ij} Q(A_{\{j\}}^t) Q(B_{\{i\}}^t | A_{\{j\}}^t) \prod_{l \in \mathcal{N}_j \setminus \{i\}} Q(X_l^t | A_{\{j\}}^t) \bar{\chi}(\Omega_{j \rightarrow i}^t | B_{\{i\}}^t A_{\{j\}}^t X_{\mathcal{N}_j \setminus \{i\}}^t) \\ &\quad - \sum_{j=1}^N \sum_{X_{\mathcal{N}_j \setminus \{i\}}} G_{ij} Q(B_{\{j\}}^t) Q(A_i | B_{\{j\}}^t) \prod_{l \in \mathcal{N}_j \setminus \{i\}} Q(X_l^t | B_{\{j\}}^t) \bar{\chi}(\Omega_{j \rightarrow i}^t | A_{\{i\}}^t B_{\{j\}}^t X_{\mathcal{N}_j \setminus \{i\}}^t). \end{aligned}$$

205 Since  $Q(B_{\{i\}}^t | A_{\{j\}}^t) = Q(B_{\{i\}}^t A_{\{j\}}^t) / Q(A_{\{j\}}^t)$ , in order to evaluate these equations we require additional  
 206 equations describing how pair probabilities change with time or some appropriate closure of pairs in terms  
 207 of single node probabilities. From the master equation we can derive exact equations describing pairs. For  
 208 the probability  $P(B_{\{i\}}^t A_{\{j\}}^t)$  we obtain

$$\begin{aligned} \frac{dP(B_{\{i\}}^t A_{\{j\}}^t)}{dt} &= \sum_{k=1}^N \sum_{X_{V \setminus \{i,j,k\}}} G_{jk} P(B_{\{i\}}^t B_{\{j\}}^t A_{\{k\}}^t X_{V \setminus \{i,j,k\}}^t) \chi(\Omega_{k \rightarrow j}^t | B_{\{i\}}^t B_{\{j\}}^t A_{\{k\}}^t X_{V \setminus \{i,j,k\}}^t) \\ &\quad - \sum_{k=1}^N \sum_{X_{V \setminus \{i,j,k\}}} G_{jk} P(B_{\{i\}}^t A_{\{j\}}^t B_{\{k\}}^t X_{V \setminus \{i,j,k\}}^t) \chi(\Omega_{k \rightarrow j}^t | B_{\{i\}}^t A_{\{j\}}^t B_{\{k\}}^t X_{V \setminus \{i,j,k\}}^t) \\ &\quad + \sum_{k=1}^N \sum_{X_{V \setminus \{i,j,k\}}} G_{ik} P(B_{\{k\}}^t A_{\{i\}}^t A_{\{j\}}^t X_{V \setminus \{i,j,k\}}^t) \chi(\Omega_{k \rightarrow i}^t | B_{\{k\}}^t A_{\{i\}}^t A_{\{j\}}^t X_{V \setminus \{i,j,k\}}^t) \\ &\quad - \sum_{k=1}^N \sum_{X_{V \setminus \{i,j,k\}}} G_{ik} P(A_{\{k\}}^t B_{\{i\}}^t A_{\{j\}}^t X_{V \setminus \{i,j,k\}}^t) \chi(\Omega_{k \rightarrow i}^t | A_{\{k\}}^t B_{\{i\}}^t A_{\{j\}}^t X_{V \setminus \{i,j,k\}}^t). \quad (9) \end{aligned}$$

209 We can now apply the same assumption regarding total fitness that we used for the single node probabilities  
 210 so that

$$\begin{aligned} \frac{dQ(B_{\{i\}}^t A_{\{j\}}^t)}{dt} &= \sum_{k=1}^N \sum_{X_{\mathcal{N}_k \setminus \{i,j\}}} G_{jk} Q(B_{\{i\}}^t B_{\{j\}}^t A_{\{k\}}^t X_{\mathcal{N}_k \setminus \{i,j\}}^t) \bar{\chi}(\Omega_{k \rightarrow j}^t | B_{\{i\}}^t B_{\{j\}}^t A_{\{k\}}^t X_{\mathcal{N}_k \setminus \{i,j\}}^t) \\ &\quad - \sum_{k=1}^N \sum_{X_{\mathcal{N}_k \setminus \{i,j\}}} G_{jk} Q(B_{\{i\}}^t A_{\{j\}}^t B_{\{k\}}^t X_{\mathcal{N}_k \setminus \{i,j\}}^t) \bar{\chi}(\Omega_{k \rightarrow j}^t | B_{\{i\}}^t A_{\{j\}}^t B_{\{k\}}^t X_{\mathcal{N}_k \setminus \{i,j\}}^t) \\ &\quad + \sum_{k=1}^N \sum_{X_{\mathcal{N}_k \setminus \{i,j\}}} G_{ik} Q(B_{\{k\}}^t A_{\{i\}}^t A_{\{j\}}^t X_{\mathcal{N}_k \setminus \{i,j\}}^t) \bar{\chi}(\Omega_{k \rightarrow i}^t | B_{\{k\}}^t A_{\{i\}}^t A_{\{j\}}^t X_{\mathcal{N}_k \setminus \{i,j\}}^t) \\ &\quad - \sum_{k=1}^N \sum_{X_{\mathcal{N}_k \setminus \{i,j\}}} G_{ik} Q(A_{\{k\}}^t B_{\{i\}}^t A_{\{j\}}^t X_{\mathcal{N}_k \setminus \{i,j\}}^t) \bar{\chi}(\Omega_{k \rightarrow i}^t | A_{\{k\}}^t B_{\{i\}}^t A_{\{j\}}^t X_{\mathcal{N}_k \setminus \{i,j\}}^t). \quad (10) \end{aligned}$$

211 Applying Bayes' Theorem to the neighbourhood probability  $Q(B_{\{i\}}^t B_{\{j\}}^t A_{\{k\}}^t X_{V \setminus \{i,j,k\}}^t)$  we obtain

$$Q(B_{\{i\}}^t B_{\{j\}}^t A_{\{k\}}^t X_{\mathcal{N}_k \setminus \{i,j\}}^t) = Q(B_{\{j\}}^t A_{\{k\}}^t) Q(B_{\{i\}}^t X_{\mathcal{N}_k \setminus \{i,j\}}^t | B_{\{j\}}^t A_{\{k\}}^t)$$

212 We can now assume statistical independence of the remaining nodes given the state of  $j$  and  $k$  so that

$$Q(B_{\{i\}}^t B_{\{j\}}^t A_{\{k\}}^t X_{\mathcal{N}_k \setminus \{i,j\}}^t) \approx Q(B_{\{j\}}^t A_{\{k\}}^t) Q(B_{\{i\}}^t | B_{\{j\}}^t A_{\{k\}}^t) \prod_{l \in \mathcal{N}_k \setminus \{i,j\}} Q(X_l^t | B_{\{j\}}^t A_{\{k\}}^t).$$

213 Since we know that node  $i$  is connected to node  $j$  we can assume that given the state of node  $j$ , the state of  
 214 node  $i$  is independent of node  $k$ , and similarly the state of any node in the neighbourhood of  $k$  is independent  
 215 of node  $j$ , which gives us

$$Q(B_{\{i\}}^t B_{\{j\}}^t A_{\{k\}}^t X_{\mathcal{N}_k \setminus \{i,j\}}^t) \approx Q(B_{\{j\}}^t A_{\{k\}}^t) Q(B_{\{i\}}^t | B_{\{j\}}^t) \prod_{l \in \mathcal{N}_k \setminus \{i,j\}} Q(X_{\{l\}}^t | A_{\{k\}}^t).$$

216 Substituting this into Equation (10) gives

$$\begin{aligned} \frac{dQ(B_{\{i\}}^t A_{\{j\}}^t)}{dt} &\approx \sum_{k=1}^N \sum_{X_{\mathcal{N}_k \setminus \{i,j\}}} G_{jk} Q(B_{\{j\}}^t A_{\{k\}}^t) Q(B_{\{i\}}^t | B_{\{j\}}^t) \prod_{l \in \mathcal{N}_k \setminus \{i,j\}} Q(X_{\{l\}}^t | A_{\{k\}}^t) \bar{\chi}(\Omega_{k \rightarrow j}^t | B_{\{i\}}^t B_{\{j\}}^t A_{\{k\}}^t X_{\mathcal{N}_k \setminus \{i,j\}}^t) \\ &- \sum_{k=1}^N \sum_{X_{\mathcal{N}_k \setminus \{i,j\}}} G_{jk} Q(A_{\{j\}}^t B_{\{k\}}^t) Q(B_{\{i\}}^t | A_{\{j\}}^t) \prod_{l \in \mathcal{N}_k \setminus \{i,j\}} Q(X_{\{l\}}^t | B_{\{k\}}^t) \bar{\chi}(\Omega_{k \rightarrow j}^t | B_{\{i\}}^t A_{\{j\}}^t B_{\{k\}}^t X_{\mathcal{N}_k \setminus \{i,j\}}^t) \\ &+ \sum_{k=1}^N \sum_{X_{\mathcal{N}_k \setminus \{i,j\}}} G_{ik} Q(A_{\{i\}}^t B_{\{k\}}^t) Q(A_{\{j\}}^t | A_{\{i\}}^t) \prod_{l \in \mathcal{N}_k \setminus \{i,j\}} Q(X_{\{l\}}^t | B_{\{k\}}^t) \bar{\chi}(\Omega_{k \rightarrow i}^t | A_{\{i\}}^t A_{\{j\}}^t B_{\{k\}}^t X_{\mathcal{N}_k \setminus \{i,j\}}^t) \\ &- \sum_{k=1}^N \sum_{X_{\mathcal{N}_k \setminus \{i,j\}}} G_{ik} Q(B_{\{i\}}^t A_{\{k\}}^t) Q(A_{\{j\}}^t | B_{\{i\}}^t) \prod_{l \in \mathcal{N}_k \setminus \{i,j\}} Q(X_{\{l\}}^t | A_{\{k\}}^t) \bar{\chi}(\Omega_{k \rightarrow i}^t | B_{\{i\}}^t A_{\{j\}}^t A_{\{k\}}^t X_{\mathcal{N}_k \setminus \{i,j\}}^t). \end{aligned}$$

217 While this system is closed, its computational complexity increases exponentially with the maximum node  
 218 degree of the graph, so it is not numerically feasible for graphs with highly connected nodes. While this  
 219 could potentially be addressed by introducing approximations for nodes with high degree and this may lead  
 220 to accurate models, here we continue towards a simplified model. To do this, we follow the same process as  
 221 in epidemic models and make a homogeneity assumption by assuming that any pair is equally likely to be  
 222 in any given state [18, 33]; i.e.  $Q(X_{\{i\}}^t | Y_{\{j\}}^t) = Q(X^t | Y^t)$  for all pairs  $(i, j)$ . This leads to

$$\begin{aligned} \frac{dQ(A_{\{i\}}^t)}{dt} &\approx \sum_{j=1}^N \sum_{X_{\mathcal{N}_j \setminus \{i\}}} G_{ij} Q(A_{\{j\}}^t) Q(B^t | A^t)^{k_j - n_X} Q(A^t | A^t)^{n_X} \bar{\chi}(\Omega_{j \rightarrow i}^t | B_{\{i\}}^t A_{\{j\}}^t X_{\mathcal{N}_j \setminus \{i\}}^t) \\ &- \sum_{j=1}^N \sum_{X_{\mathcal{N}_j \setminus \{i\}}} G_{ij} Q(B_{\{j\}}^t) Q(A^t | B^t)^{n_X + 1} Q(B^t | B^t)^{k_j - n_X - 1} \bar{\chi}(\Omega_{j \rightarrow i}^t | A_{\{i\}}^t B_{\{j\}}^t X_{\mathcal{N}_j \setminus \{i\}}^t), \end{aligned}$$

223 where  $k_j$  is the degree of node  $j$  and  $n_X$  is the number of type  $A$  individuals in state  $X_{\mathcal{N}_j \setminus \{i\}}$ . Since the  
 224 transition rate only depends on the number of type  $A$  and type  $B$  individuals in the neighbourhood of node  
 225  $j$  and not on their positions, the summand on the right hand side is equal for all states  $X_{\mathcal{N}_j \setminus \{i\}}$  which have  
 226 the same configuration of  $A$  and  $B$  individuals. The frequency of a certain neighbourhood state across all  
 227 possible configurations is given by the binomial coefficient, so that

$$\begin{aligned} \frac{dQ(A_{\{i\}}^t)}{dt} &\approx \sum_{j=1}^N \sum_{n=0}^{k_j-1} G_{ij} \binom{k_j-1}{n} Q(A_{\{j\}}^t) Q(B^t | A^t)^{k_j - n + 1} Q(A^t | A^t)^n \bar{\chi}(\Omega_{j \rightarrow i}^t | n) \\ &- \sum_{j=1}^N \sum_{n=0}^{k_j-1} G_{ij} \binom{k_j-1}{n} Q(B_{\{j\}}^t) Q(A^t | B^t)^{n+1} Q(B^t | B^t)^{k_j - n} \bar{\chi}(\Omega_{j \rightarrow i}^t | n), \end{aligned}$$

228 where  $\bar{\chi}(\Omega_{A \rightarrow B}^t | n)$  is the rate at which we select one of the type  $A$  individuals to reproduce and replace a  
 229 type  $B$ , given that there are  $n$  type  $A$  individuals and  $k_j - n$  type  $B$  individuals in the neighbourhood of  
 230 the selected node.

231 Since we have assumed that any pair is equally likely, this assumption only holds when every node in the  
 232 graph forms  $k$  connections, which are chosen at random. Therefore we require that node  $i$  is equally likely  
 233 to be connected to any other node and all nodes are topologically equivalent, so that the probability that a  
 234 given node of type  $B$  is connected to  $x$  type  $A$  neighbours is given by a binomial distribution with  $n = k$   
 235 and  $p = Q(A^t|B^t)$ . Therefore the probability of an individual being type  $A$  changes with rate

$$\begin{aligned} \frac{dQ(A^t)}{dt} &\approx \sum_{x=0}^k \binom{k}{x} Q(A^t|B^t)^x Q(B_t|B_t)^{k-x} Q(B^t)^x \sum_{n=0}^{k-1} \binom{k-1}{n} Q(B^t|A^t)^{k-n+1} Q(A^t|A^t)^n \bar{\chi}(\Omega_{A \rightarrow B}^t|n) \\ &\quad - \sum_{x=0}^k \binom{k}{x} Q(A^t|A^t)^x Q(B_t|A_t)^{k-x} Q(A^t)^x (k-x) \sum_{n=0}^{k-1} \binom{k-1}{n} Q(A^t|B^t)^{n+1} Q(B^t|B^t)^{k-n} \bar{\chi}(\Omega_{B \rightarrow A}^t|n). \end{aligned}$$

236 We can also apply these assumptions to the pair-level equations to obtain a closed system of equations  
 237 which are efficient to solve numerically. The resulting model is equivalent to the model in [26], which was  
 238 justified by using the assumption that the population occupies a regular graph, such that all individuals  
 239 have degree  $k$ , and that all nodes are topologically equivalent, such that every pair of individuals is equally  
 240 likely to be connected. We have shown that by applying these assumptions to the exact node-level equations  
 241 (Equation (4)) we can derive these models.

242 Similarly we can obtain a pair approximation model for the dynamics where we select on death by  
 243 conditioning against the state of the neighbours of node  $i$ . Applying analogous assumptions to the previous  
 244 example then leads to the model in [8]. These models have been shown to yield interesting qualitative  
 245 results about the relative strengths of different strategies in evolutionary games on graphs. However, the  
 246 homogeneity assumptions made result in losing important aspects of the structure, such as how individual  
 247 nodes in the system can behave differently. In the next sections we will attempt to develop approximation  
 248 methods which can capture this node-specific information.

249 As we alluded to earlier, a natural method would be to use Equation (7) as a basis for this. However,  
 250 difficulties in implementing this method on general networks as well as the number of equations that result  
 251 leads us to a different direction for the present work.

### 252 3.2. An unconditioned fitness approximation model

253 Here we develop a method which removes the need to include the probability of whole neighbourhoods  
 254 by removing the conditioning in the replacement rate. This causes the replacement rate to only depend on  
 255 the marginal probabilities of the state of each node rather than the full system state. This assumption also  
 256 motivated a model in [37] in which the authors construct a population-level approximation describing how  
 257 the expected number of individuals of each type change with time. Under this assumption, Equation (4)  
 258 becomes

$$\frac{dP(A_{\{i\}}^t)}{dt} \approx \sum_{j=1}^N \sum_{X_{V \setminus \{i,j\}}} G_{ij} P(B_{\{i\}}^t A_{\{j\}}^t X_{V \setminus \{i,j\}}^t) \chi(\Omega_{j \rightarrow i}^t) - \sum_{j=1}^N \sum_{X_{V \setminus \{i,j\}}} G_{ij} P(A_{\{i\}}^t B_{\{j\}}^t X_{V \setminus \{i,j\}}^t) \chi(\Omega_{j \rightarrow i}^t).$$

259 Since  $\chi(\Omega_{j \rightarrow i}^t)$  is now the same for all system states,

$$\frac{dP(A_{\{i\}}^t)}{dt} \approx \sum_{j=1}^N G_{ij} P(B_{\{i\}}^t A_{\{j\}}^t) \chi(\Omega_{j \rightarrow i}^t) - \sum_{j=1}^N G_{ij} P(A_{\{i\}}^t B_{\{j\}}^t) \chi(\Omega_{j \rightarrow i}^t).$$

260 Adding and subtracting  $\sum_{j=1}^N G_{ij} P(A_{\{i\}}^t A_{\{j\}}^t) \chi(\Omega_{j \rightarrow i}^t)$  we obtain

$$\begin{aligned}
\frac{dP(A_{\{i\}}^t)}{dt} &\approx \sum_{j=1}^N \left[ G_{ij} \bar{P}(B_{\{i\}}^t A_{\{j\}}^t) \chi(\Omega_{j \rightarrow i}^t) + G_{ij} P(A_{\{i\}}^t A_{\{j\}}^t) \chi(\Omega_{j \rightarrow i}^t) \right] \\
&\quad - \sum_{j=1}^N \left[ G_{ij} P(A_{\{i\}}^t B_{\{j\}}^t) \chi(\Omega_{j \rightarrow i}^t) + G_{ij} \bar{P}(A_{\{i\}}^t A_{\{j\}}^t) \chi(\Omega_{j \rightarrow i}^t) \right] \\
&\approx \sum_{j=1}^N G_{ij} P(A_{\{j\}}^t) \chi(\Omega_{j \rightarrow i}^t) - \sum_{j=1}^N G_{ij} P(A_{\{i\}}^t) \chi(\Omega_{j \rightarrow i}^t),
\end{aligned}$$

261 which is a closed set of  $N$  equations with at most  $N$  summands on the right hand side. Therefore by defining  
262  $\bar{P}$  as an approximation to the probability distribution  $P$  we obtain the closed system

$$\frac{d\bar{P}(A_{\{i\}}^t)}{dt} = \sum_{j=1}^N G_{ij} \bar{P}(A_{\{j\}}^t) \chi(\Omega_{j \rightarrow i}^t) - \sum_{j=1}^N G_{ij} \bar{P}(A_{\{i\}}^t) \chi(\Omega_{j \rightarrow i}^t), \quad (11)$$

263 which is easy to solve numerically for an arbitrary graph.

264 **Example 3.1** (Neutral drift). *In the special case of neutral drift, i.e. when all individuals have identical*  
265 *fitness, the unconditioned fitness model gives the exact fixation probability. With the dynamics of the invasion*  
266 *process under neutral drift we obtain  $\chi(\Omega_{j \rightarrow i}^t) = \frac{1}{Nk_j}$ , and therefore Equation (11) can be written as*

$$\frac{d\bar{P}(A_{\{i\}}^t)}{dt} = \sum_{j=1}^N G_{ij} \bar{P}(A_{\{j\}}^t) \frac{1}{Nk_j} - \sum_{j=1}^N G_{ij} \bar{P}(A_{\{i\}}^t) \frac{1}{Nk_j},$$

267 *which is equivalent to the exact node equation (4) for the invasion process under neutral drift [32]. The*  
268 *unconditioned fitness model is also exact for all update mechanisms under neutral drift, but we do not write*  
269 *the equations explicitly here.*

270 As the population size  $N$  increases, the solution to Equation (11) moves further away from the exact  
271 fixation probability obtained either by solving the master equation (3) or from the output of stochastic  
272 simulations. To obtain a reasonable approximation to the fixation probability from a given initial condition  
273 we construct a scaling factor for the constant fitness case by comparing the ratio between the solution of  
274 Equation (11) on a complete graph to the exact fixation probability on a complete graph. We choose the  
275 complete graph because the exact fixation probability can be calculated analytically in this case. Whilst we  
276 consider the constant fitness case, it may also be possible to find a suitable scaling factor in the frequency  
277 dependent fitness case, however using a complete graph may no longer be appropriate because the relative  
278 strength of different strategies in some games is strongly affected by the average degree of the graph [28].

279 **Example 3.2** (Invasion process). *For constant fitness under the dynamics of the invasion process, the*  
280 *exact fixation probability for  $m$  initial mutant  $A$  individuals on a complete graph is equivalent to the Moran*  
281 *probability [20]:*

$$\rho = \frac{1 - \frac{1}{r^m}}{1 - \frac{1}{r^N}}.$$

282 *Since the fixation probability is known, we now need to solve Equation (11) on the complete graph to*  
283 *derive the ratio between the two. In the constant fitness case this can be done analytically, with the scaling*  
284 *factor for  $m$  initial mutants given by*

$$\frac{\rho}{\lim_{t \rightarrow \infty} A_c(t)} = \frac{\frac{1 - \frac{1}{r^m}}{1 - \frac{1}{r^N}}}{\frac{1}{r-1} \left( -1 + \sqrt{1 + \frac{m(r^2-1)}{N}} \right)}, \quad (12)$$

285 where  $A_c(t) = \frac{1}{N} \sum_{j=1}^N \bar{P}(A_{\{j\}}^t)$ . The derivation of this can be found in Appendix B.

286 We can now define two methods for predicting the fixation probability under any Markovian update  
287 mechanism.

288 • **Method 1** (Unconditioned fitness model) Solve Equation (11) to provide an approximation to the  
289 dynamics of the evolutionary process. (see supplementary code for the unconditioned fitness model  
290 solver)

291 • **Method 2** (Scaled unconditioned fitness model) Solve Equation (11) and then use a scaling factor,  
292 the ratio of the exact fixation probability and the solution to Equation (11) for the complete graph, to  
293 provide an approximation to the fixation probability from a given initial condition.

294 In Section 4 we investigate the numerical performance of these two methods. Note that for the purpose of this  
295 paper we have found the scaling factor for Method 2 under the invasion process (Equation (12)). However,  
296 the method can be applied to other update mechanisms, such as death-birth with selection on birth, by  
297 finding an appropriate scaling factor, which can be done by solving Equation (11) (either analytically or  
298 numerically) and comparing to the exact fixation probability on the complete graph. For example, see [12]  
299 for the exact fixation probability on a complete graph under the DB-B dynamics.

### 300 3.3. A contact conditioning approximation model

301 In Section 3.2 we restricted the conditioning so that we only require the marginal probabilities of the  
302 individual nodes. However, this removes a significant amount of information from the dynamics. In the  
303 evolutionary process, when considering a replacement event the two nodes of most interest are the node  
304 selected for birth and the node selected for death. Therefore, here we follow a similar method but retain  
305 conditioning on the states of these two key nodes. Since we restrict the conditioning to only the states of  
306 the relevant contact, when looking at the term  $\chi(\Omega_{j \rightarrow i}^t | B_{\{i\}}^t A_{\{j\}}^t X_{V \setminus \{i,j\}}^t)$  in Equation (4) we condition only  
307 on the states of the nodes  $i$  and  $j$  and obtain

$$\chi(\Omega_{j \rightarrow i}^t | B_{\{i\}}^t A_{\{j\}}^t X_{V \setminus \{i,j\}}^t) \approx \chi(\Omega_{j \rightarrow i}^t | B_{\{i\}}^t A_{\{j\}}^t).$$

308 Under the above condition, Equation (4) becomes

$$\begin{aligned} \frac{dP(A_{\{i\}}^t)}{dt} &\approx \sum_{j=1}^N \sum_{X_{V \setminus \{i,j\}}} G_{ij} P(B_{\{i\}}^t A_{\{j\}}^t X_{V \setminus \{i,j\}}^t) \chi(\Omega_{j \rightarrow i}^t | B_{\{i\}}^t A_{\{j\}}^t) \\ &\quad - \sum_{j=1}^N \sum_{X_{V \setminus \{i,j\}}} G_{ij} P(A_{\{i\}}^t B_{\{j\}}^t X_{V \setminus \{i,j\}}^t) \chi(\Omega_{j \rightarrow i}^t | A_{\{i\}}^t B_{\{j\}}^t). \end{aligned} \quad (13)$$

309 To see the effect of this assumption on the rates, consider  $\chi(\Omega_{j \rightarrow i}^t | B_{\{i\}}^t A_{\{j\}}^t)$ . Here we condition only against  
310 node  $i$  being in state  $B$  and node  $j$  being in state  $A$  rather than against the entire system state. Consequently  
311 in the fitness equation (6) we have  $P(B_{\{i\}}^t) = 1$  and  $P(A_{\{j\}}^t) = 1$  giving

$$f_j^t | B_{\{i\}}^t A_{\{j\}}^t = f_{back} + w \frac{bT_{ij} + a \sum_{l \neq i} G_{jl} P(A_{\{l\}}^t) + b \sum_{l \neq i} G_{jl} P(B_{\{l\}}^t)}{\sum_{l=1}^N G_{jl}}.$$

312 In Equation (13), the chance of selecting node  $j$  is now independent of the state  $X_{V \setminus \{i,j\}}^t$  of the remaining  
313 nodes which enables the equation to be reduced to

$$\frac{dP(A_{\{i\}}^t)}{dt} \approx \sum_{j=1}^N G_{ij} P(B_{\{i\}}^t A_{\{j\}}^t) \chi(\Omega_{j \rightarrow i}^t | B_{\{i\}}^t A_{\{j\}}^t) - \sum_{j=1}^N G_{ij} P(A_{\{i\}}^t B_{\{j\}}^t) \chi(\Omega_{j \rightarrow i}^t | A_{\{i\}}^t B_{\{j\}}^t). \quad (14)$$

314 This gives an approximate equation for individuals in terms of pairs. We then need to build equations to  
 315 describe pair-level probabilities. Similar methodologies have been followed to describe epidemics propagated  
 316 on networks [33, 34].

317 Applying the same conditioning to the exact pair level equation (9) we obtain

$$\begin{aligned} \frac{dP(B_{\{i\}}^t A_{\{j\}}^t)}{dt} &\approx \sum_{k=1}^N G_{jk} P(B_{\{i\}}^t B_{\{j\}}^t A_{\{k\}}^t) \chi(\Omega_{k \rightarrow j}^t | B_{\{j\}}^t A_{\{k\}}^t) - \sum_{k=1}^N G_{jk} P(B_{\{i\}}^t A_{\{j\}}^t B_{\{k\}}^t) \chi(\Omega_{k \rightarrow j}^t | A_{\{j\}}^t B_{\{k\}}^t) \\ &+ \sum_{k=1}^N G_{ik} P(B_{\{k\}}^t A_{\{i\}}^t A_{\{j\}}^t) \chi(\Omega_{k \rightarrow i}^t | B_{\{k\}}^t A_{\{i\}}^t) - \sum_{k=1}^N G_{ik} P(A_{\{k\}}^t B_{\{i\}}^t A_{\{j\}}^t) \chi(\Omega_{k \rightarrow i}^t | A_{\{k\}}^t B_{\{i\}}^t). \end{aligned} \quad (15)$$

318 Similar formulae can be constructed for all possible pairs, writing pairs in terms of triples. In a sim-  
 319 ilar way, triples can be written in terms of quads and so on, up to the full system size  $N$  which is  
 320 then closed. Therefore, when using this method we obtain a hierarchy similar to the BBGKY (Bogoli-  
 321 ubov–Born–Green–Kirkwood–Yvon) hierarchy [4, 16] in statistical physics. However, here the hierarchy  
 322 only represents an approximation to the original dynamics. Solving this system exactly is no simpler than  
 323 evaluating Equation (3) since evaluating the hierarchy in full is comparable in numerical complexity, so we  
 324 wish to find approximation methods to reduce this.

325 With this hierarchy, we can apply techniques developed in statistical physics to approximate higher-  
 326 order terms as functions of lower-order terms. In particular we can close the system of equations (14)  
 327 and (15) at the level of pairs by approximating all triples in Equation (15) in terms of pair-level and  
 328 individual-level probabilities. Similar techniques have been applied for many stochastic processes including  
 329 in epidemiology [14, 18, 33, 34] and evolutionary dynamics [10, 28, 37] leading to models which can be  
 330 numerically evaluated.

331 To close the system, we require a functional form that can approximate triple probabilities in terms of  
 332 individual and pair probabilities. One method is to approximate a triple  $P(A_{\{i\}}^t B_{\{j\}}^t C_{\{k\}}^t)$  as the product of  
 333 all possible pairs among these nodes divided by the product of all individuals, i.e.

$$P(A_{\{i\}}^t B_{\{j\}}^t C_{\{k\}}^t) \approx \frac{P(A_{\{i\}}^t B_{\{j\}}^t) P(B_{\{j\}}^t C_{\{k\}}^t) P(A_{\{i\}}^t C_{\{k\}}^t)}{P(A_{\{i\}}^t) P(B_{\{j\}}^t) P(C_{\{k\}}^t)}. \quad (16)$$

334 This closure is commonly attributed to Kirkwood [36] because it is derived from the Kirkwood superposition  
 335 which approximates triples in terms of pairs in thermodynamics [15, 17]. This is often applied to nodes  $i, j, k$   
 336 that form a 3-cycle in the graph, which we call a ‘closed triple’, although it can be applied to any triplet  
 337 of nodes. It has been shown that this closure maximises the entropy of these thermodynamic systems [36],  
 338 and it also ensures that symmetry is preserved across the triplet. This closure has commonly been adapted  
 339 to probabilistic systems, such as the BBGKY hierarchy [4, 16] and epidemic modelling [13, 33, 35]. How-  
 340 ever, the Kirkwood closure for probabilities does not define a probability distribution since we can obtain  
 341  $P(B_{\{i\}}^t A_{\{j\}}^t) + P(B_{\{i\}}^t B_{\{j\}}^t) \neq P(B_{\{i\}}^t)$ , which has been observed numerically [31]. In spite of this it has  
 342 been shown to yield accurate approximations in these probabilistic systems [31, 33, 36].

343 Another closure can be obtained by applying Bayes’ Theorem and assuming statistical independence  
 344 across the triple given the state of the central node, in this case node  $j$ . By applying Bayes’ Theorem we  
 345 have

$$P(A_{\{i\}}^t B_{\{j\}}^t C_{\{k\}}^t) = P(A_{\{i\}}^t | B_{\{j\}}^t C_{\{k\}}^t) P(B_{\{j\}}^t C_{\{k\}}^t),$$

346 which, when we assume statistical independence of nodes  $i$  and  $k$  given  $j$ , simplifies to

$$P(A_{\{i\}}^t B_{\{j\}}^t C_{\{k\}}^t) \approx P(A_{\{i\}}^t | B_{\{j\}}^t) P(B_{\{j\}}^t C_{\{k\}}^t) = \frac{P(A_{\{i\}}^t B_{\{j\}}^t) P(B_{\{j\}}^t C_{\{k\}}^t)}{P(B_{\{j\}}^t)}. \quad (17)$$

347 Typically this closure is applied to nodes on a graph where nodes  $i$  and  $j$  are connected and nodes  $j$  and  
 348  $k$  are connected but where there is no connection between nodes  $i$  and  $k$ , which we call an ‘open triple’.

349 However, it could be applied to any triplet of nodes. This closure method is thought to be most accurate on  
 350 trees [18, 31, 34], and has been shown to be exact for such graphs under the SIR epidemic model [19, 34, 35].

351 We can adopt either closure to remove triples and close the system. For example, if we are using the  
 352 Kirkwood closure to approximate all triples in Equation (15) we obtain the system of equations

$$\begin{aligned}
 \frac{d\bar{P}(A_{\{i\}}^t)}{dt} &= \sum_{j=1}^N G_{ij} \bar{P}(B_{\{i\}}^t A_{\{j\}}^t) \chi(\Omega_{j \rightarrow i}^t | B_{\{i\}}^t A_{\{j\}}^t) - \sum_{j=1}^N G_{ij} \bar{P}(A_{\{i\}}^t B_{\{j\}}^t) \chi(\Omega_{j \rightarrow i}^t | A_{\{i\}}^t B_{\{j\}}^t). \\
 \frac{d\bar{P}(B_{\{i\}}^t A_{\{j\}}^t)}{dt} &= \sum_{k=1}^N G_{jk} \frac{\bar{P}(B_{\{i\}}^t B_{\{j\}}^t) \bar{P}(B_{\{j\}}^t A_{\{k\}}^t) \bar{P}(B_{\{i\}}^t A_{\{k\}}^t)}{\bar{P}(B_{\{i\}}^t) \bar{P}(B_{\{j\}}^t) \bar{P}(A_{\{k\}}^t)} \chi(\Omega_{k \rightarrow j}^t | B_{\{j\}}^t A_{\{k\}}^t) \\
 &\quad - \sum_{k=1}^N G_{jk} \frac{\bar{P}(B_{\{i\}}^t A_{\{j\}}^t) \bar{P}(A_{\{j\}}^t B_{\{k\}}^t) \bar{P}(B_{\{i\}}^t B_{\{k\}}^t)}{\bar{P}(B_{\{i\}}^t) \bar{P}(A_{\{j\}}^t) \bar{P}(B_{\{k\}}^t)} \chi(\Omega_{k \rightarrow j}^t | A_{\{j\}}^t B_{\{k\}}^t) \\
 &\quad + \sum_{k=1}^N G_{ik} \frac{\bar{P}(B_{\{k\}}^t A_{\{i\}}^t) \bar{P}(A_{\{i\}}^t A_{\{j\}}^t) \bar{P}(B_{\{k\}}^t A_{\{j\}}^t)}{\bar{P}(B_{\{k\}}^t) \bar{P}(A_{\{i\}}^t) \bar{P}(A_{\{j\}}^t)} \chi(\Omega_{k \rightarrow i}^t | B_{\{k\}}^t A_{\{i\}}^t) \\
 &\quad - \sum_{k=1}^N G_{ik} \frac{\bar{P}(A_{\{k\}}^t B_{\{i\}}^t) \bar{P}(B_{\{i\}}^t A_{\{j\}}^t) \bar{P}(A_{\{k\}}^t A_{\{j\}}^t)}{\bar{P}(A_{\{k\}}^t) \bar{P}(B_{\{i\}}^t) \bar{P}(A_{\{j\}}^t)} \chi(\Omega_{k \rightarrow i}^t | A_{\{k\}}^t B_{\{i\}}^t),
 \end{aligned}$$

353 where  $\bar{P}$  represents the approximation to the probability distribution  $P$ . However, note that using this  
 354 closure for all triples will eventually require equations for every pair of nodes in the system, whether they  
 355 are connected or not.

356 It is also useful to use a combination of the two methods whereby the Kirkwood closure (16) is used for  
 357 closed triples, and (17) is used for open triples [13, 33]. In this work we shall use this combined approach  
 358 to obtain a closed system. However, we find that unlike in epidemiology, this standard approach does not  
 359 produce good results. We therefore also try using just the Kirkwood closure because this permits explicit  
 360 correlations between nodes which are not linked, although as indicated above, this substantially increases  
 361 computational complexity because the system of equations will scale with  $N^2$  rather than the number of  
 362 connected individuals in the graph.

363 With the contact conditioning model we define two different methods to approximate the evolutionary  
 364 dynamics.

- 365 • **Method 3** (Open and closed triples) Solve Equation (14) together with equations for pairs by using  
 366 two different closures for different types of triples. First consider a triple  $P(A_{\{i\}}^t B_{\{j\}}^t Z_{\{k\}}^t)$ ,  $Z \in \{A, B\}$ ,  
 367 where there is no link between nodes  $i$  and  $k$ . We call this an open triple, and can approximate it as

$$P(A_{\{i\}}^t B_{\{j\}}^t Z_{\{k\}}^t) \approx \frac{P(A_{\{i\}}^t B_{\{j\}}^t) P(B_{\{j\}}^t Z_{\{k\}}^t)}{P(B_{\{j\}}^t)}.$$

368 If there exists a link between nodes  $i$  and  $k$  we call this a closed triple, and approximate this using the  
 369 Kirkwood closure,

$$P(A_{\{i\}}^t B_{\{j\}}^t Z_{\{k\}}^t) \approx \frac{P(A_{\{i\}}^t B_{\{j\}}^t) P(B_{\{j\}}^t Z_{\{k\}}^t) P(A_{\{i\}}^t Z_{\{k\}}^t)}{P(A_{\{i\}}^t) P(B_{\{j\}}^t) P(Z_{\{k\}}^t)}.$$

370 Using this method it is only necessary to use pairs which have a link between them in the graph, and  
 371 so it scales with  $Nd$ , where  $d$  is the average degree of the graph.

- 372 • **Method 4** (Kirkwood closure only) Solve Equation (14) together with equations for pairs by using  
 373 the Kirkwood closure for all triples. That is, we approximate any triple  $P(A_{\{i\}}^t B_{\{j\}}^t Z_{\{k\}}^t)$ ,  $Z \in \{A, B\}$   
 374 as

$$P(A_{\{i\}}^t B_{\{j\}}^t Z_{\{k\}}^t) \approx \frac{P(A_{\{i\}}^t B_{\{j\}}^t) P(B_{\{j\}}^t Z_{\{k\}}^t) P(A_{\{i\}}^t Z_{\{k\}}^t)}{P(A_{\{i\}}^t) P(B_{\{j\}}^t) P(Z_{\{k\}}^t)}.$$

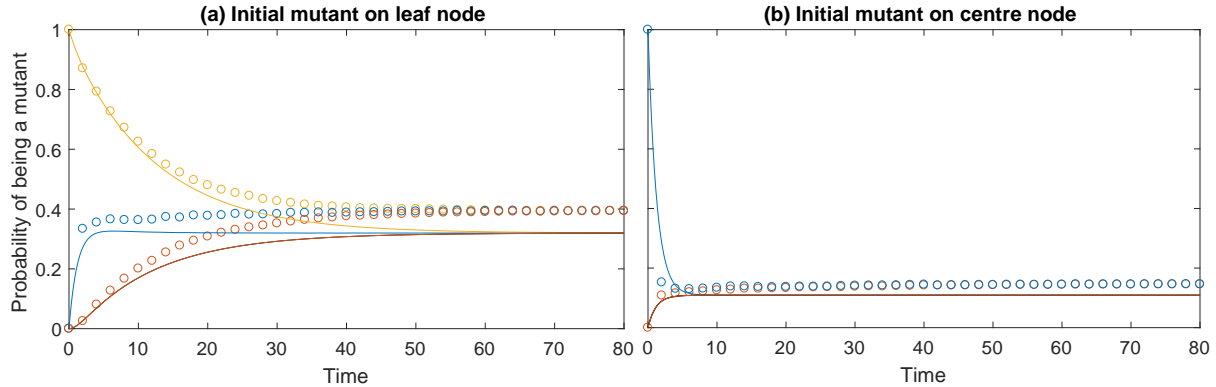


**Figure 1:** Comparison of the marginal probabilities for each node on the graph being a mutant  $A$  plotted against time as given by Method 1 (solid lines) versus stochastic simulation of the discrete-time system (circles), when applied to the invasion process on a 4-node star graph. We consider (a) dynamics initiated with a single  $A$  individual on a leaf node and (b) dynamics initiated with a single  $A$  individual on the central node. Each line represents the marginal probability of a certain node in the graph being occupied by an  $A$  individual, the corresponding colours between solid lines and circles represent the same node on the graph. The stochastic process is simulated 10,000 times from the same initial condition until fixation of either the mutant or resident strategy. The probabilities represent, for a given node at a given time, the proportion of simulations for which that node is a mutant. Method 1 is numerically integrated to approximate the probability of each node being a mutant at a given time. This is the constant fitness case where  $A$  individuals have fitness 1.2 and  $B$  individuals have fitness 1.

375 This method requires the use of every pair of nodes in the system, not just those which are directly  
 376 connected, and so scales with  $N^2$ . (see supplementary code for the constant conditioning model solver)

## 377 4. Results

### 378 4.1. A comparison of the different methods: fixation probabilities for constant fitness

379 Here we investigate the fixation probability of a single initial  $A$  individual placed in a given node on  
 380 the graph under the dynamics of the invasion process. Figure 1 compares Method 1 (unconditioned fitness  
 381 model) under the invasion process against stochastic simulation on a four-node star graph. On such small  
 382 graphs, Method 1 appears to provide a reasonable approximation to the expected dynamics and to the  
 383 fixation probability. However, for such small populations exact solutions are easy to obtain, and hence we  
 384 want to test larger population sizes. When the population size is increased, this method fails to accurately  
 385 predict the fixation probability, appearing to tend towards zero with increasing population size (for example,  
 386 see Table 1, where it can be seen that increasing the size from 20 to 35 to 50 moves the solution closer to  
 387 zero on random graphs). To account for this, we use Method 2 (scaled unconditioned fitness model).

388 Method 2 represents a scaling of the approximation from Method 1 where the scaling is derived ana-  
 389 lytically from the fixation probability for a complete graph. Consequently, it makes sense to only consider  
 390 the approximation of the fixation probability rather than the whole time series. Predictions of the fixation  
 391 probability of a single  $A$  individual when placed on various graphs using the different approximation methods  
 392 are shown in Tables 1 and 2. We first observe that the accuracy of the method does not significantly differ  
 393 for different population sizes, so this overcomes the issue with Method 1. For both the Erdős-Rényi [7]  
 394 and scale-free random graphs, we start the process in three different initial conditions; a high-degree initial  
 395 node, a low-degree initial node and an average degree initial node. This is because under the dynamics of  
 396 the invasion process, a low degree node is known to act as an amplifier of selection and a high degree node  
 397 is known to act as a suppressor [2, 32], and so we potentially expect different performance of the methods  
 398 when initiated from nodes of different degree. In the  $k$ -regular random graph, since all nodes have equal  
 399 degree, we only consider results for one initial node. In addition to the random graphs (Table 2), we also  
 400 investigate a star graph, a square lattice and Zachary’s karate club [41], which is an example of a real-world  
 401 network consisting of 34 individuals and average degree of 4.6. On these graphs we initiate the dynamics

**Table 1:** The fixation probability starting from a single mutant  $A$  individual placed on a specific node on single realisations of random graphs. To evaluate the fixation probability using the approximate methods, we solved them until a steady state was reached and calculated the average probability of a node being a mutant (the methods do not always give exactly the same value for each node). We compare this to the fixation probability as calculated by the proportion of 10,000 stochastic simulations in which the type  $A$  individuals fixated. Constant fitness is assumed, where  $A$  individuals have fitness 1.2 and  $B$  individuals have fitness 1. All graphs were generated to have an average degree of 5.

Graph	Fixation probability				
	Method 1	Method 2	Method 3	Method 4	Simulation
20 node Erdős-Rényi - initial degree 10	0.0193	0.0604	1.0000	0.0654	0.0784
20 node Erdős-Rényi - initial degree 2	0.1055	0.3301	1.0000	0.2874	0.3098
20 node Erdős-Rényi - initial degree 5	0.0424	0.1326	1.0000	0.1343	0.1575
20 node scale-free - initial degree 10	0.0190	0.0594	1.0000	0.0681	0.0783
20 node scale-free - initial degree 2	0.0945	0.2956	1.0000	0.3004	0.3153
20 node scale-free - initial degree 5	0.0475	0.1486	1.0000	0.1490	0.1606
20 node $k$ -regular	0.0547	0.1711	1.0000	0.1516	0.1722
35 node Erdős-Rényi - initial degree 10	0.0126	0.0671	1.0000	0.0782	0.0940
35 node Erdős-Rényi - initial degree 2	0.0628	0.3346	1.0000	0.3255	0.3191
35 node Erdős-Rényi - initial degree 5	0.0315	0.1679	1.0000	0.1572	0.1730
35 node scale-free - initial degree 10	0.0089	0.0474	1.0000	0.0844	0.0724
35 node scale-free - initial degree 2	0.0444	0.2366	1.0000	0.4743	0.2929
35 node scale-free - initial degree 5	0.0223	0.1188	1.0000	0.1950	0.1546
35 node $k$ -regular	0.0313	0.1668	1.0000	0.1631	0.1750
50 node Erdős-Rényi - initial degree 10	0.0083	0.0630	1.0000	0.0787	0.0820
50 node Erdős-Rényi - initial degree 2	0.0332	0.2521	1.0000	0.4175	0.3060
50 node Erdős-Rényi - initial degree 5	0.0272	0.2065	1.0000	0.2275	0.2120
50 node scale-free - initial degree 10	0.0056	0.0425	1.0000	0.0872	0.0660
50 node scale-free - initial degree 2	0.0307	0.2331	1.0000	0.3912	0.2840
50 node scale-free - initial degree 5	0.0154	0.1169	1.0000	0.1868	0.1530
50 node $k$ -regular	0.0219	0.1667	1.0000	0.1533	0.1640

402 from a high degree and low degree node. We observe that Method 2 performs best on the  $k$ -regular random  
403 graph and that generally it performs very well on any graph that does not strongly amplify or suppress the  
404 average fixation probability compared to the Moran probability, such as the Erdős-Rényi random graph and  
405 the square lattice. However on graphs which amplify (or suppress) average fixation probability, such as the  
406 scale-free random graph, the approximation becomes less accurate. On the star graph, which significantly  
407 amplifies the fixation probability, the approximation is very far from the true value. This is unsurprising  
408 because Method 2 is constructed to give the exact fixation probability on complete graphs. For Zachary's  
409 karate club, Method 2 provides a reasonable approximation, but does not capture the strong amplifying  
410 effect of the low degree node.

411 In order to improve upon the accuracy of Method 2 we developed the contact conditioning model to  
412 retain more information from the system. The contact conditioning model yields a hierarchy which offers no  
413 useful reduction in computational complexity, compared to the master equation (4). Therefore we developed  
414 Method 3 (open and closed triples approximation), analogous to closures used in epidemiology. However,  
415 through numerical evaluation we found that this only yields good approximations for simple graphs, such as  
416 line graphs and complete graphs for which we have exact analytic results in any case. On other graphs, the  
417 fixation probability approximation is equal to 1 (Tables 1 and 2) for an advantageous mutant of type  $A$ , and  
418 so this method is not particularly informative.

419 While the specific reason for this convergence to 1 (or 0 if the mutant is disadvantageous) is unclear, it  
420 seems likely that it is associated with graph-wide correlations caused by having two absorbing states. To  
421 address this we developed Method 4 (Kirkwood closure only). Through testing multiple graphs we observe  
422 (Tables 1 and 2) that the best results are obtained on Erdős-Rényi and regular random graphs, with some  
423 accuracy lost on scale-free random graphs. We observe that on the 20 node star graph, inaccuracies result

**Table 2:** The fixation probability starting from a single mutant  $A$  individual placed on a specific node on the example graphs. To evaluate the fixation probability using the approximate methods, we solved them until a steady state was reached and calculated the average probability of a node being a mutant (the methods do not always give exactly the same value for each node). We compare this to the fixation probability as calculated by the proportion of 10,000 stochastic simulations in which the type  $A$  individuals fixated. Constant fitness is assumed, where  $A$  individuals have fitness 1.2 and  $B$  individuals have fitness 1.

Graph	Fixation probability				
	Method 1	Method 2	Method 3	Method 4	Simulation
20 node star - initial degree 1	0.0574	0.1796	1.0000	0.3801	0.2895
20 node star - initial degree 19	0.0030	0.0094	1.0000	0.0217	0.0184
25 node square lattice - initial degree 2	0.0662	0.2546	1.0000	0.1532	0.2388
25 node square lattice - initial degree 4	0.0332	0.1277	1.0000	0.0780	0.1444
34 node Zachary's karate club - initial degree 2	0.0482	0.2498	1.0000	0.4285	0.3160
34 node Zachary's karate club - initial degree 16	0.0061	0.0314	1.0000	0.0461	0.0450
36 node star - initial degree 1	0.0322	0.1717	1.0000	1.0000	0.2971
36 node star - initial degree 35	0.0009	0.0051	1.0000	0.0209	0.0090
36 node square lattice - initial degree 2	0.0483	0.2646	1.0000	0.1363	0.2462
36 node square lattice - initial degree 4	0.0242	0.1326	1.0000	0.0689	0.1385
49 node star - initial degree 1	0.0224	0.1697	1.0000	1.0000	0.3070
49 node star - initial degree 48	0.0005	0.0035	1.0000	0.0260	0.0059
49 node square lattice - initial degree 2	0.0367	0.2734	1.0000	0.1241	0.2494
49 node square lattice - initial degree 4	0.0184	0.1369	1.0000	0.0609	0.1477

424 in a significantly amplified approximation when initiated on the low degree leaf nodes, and for the 35 and  
425 50 node star graphs the approximations initiated on the leaf node are close to 1. This is potentially due  
426 to the time to convergence on large stars being very long, which allows these inaccuracies to compound so  
427 that the system converges to this uninformative solution. This failure does not occur on these stars if we  
428 reduce the fitness advantage, suggesting that as the size of the star becomes very large the method will only  
429 work under weak selection. On random graphs, which do not significantly amplify fixation, this issue is also  
430 observed, but only when the fitness advantage of one type is sufficiently high. This issue starts when the  
431 fitness advantage is at about 50%, below which the solution converges to intermediate values on all random  
432 graphs tested. In addition to testing the star graph as an example of an extreme structure, we also tested  
433 a square lattice of various sizes, on which we find that Method 4 significantly underestimates the fixation  
434 probability. The square lattice is considered as an extreme scenario for this method because it contains  
435 many short cycles of order four, for which the correlations are not explicitly captured by the Kirkwood  
436 closure, which describes triples. Presenting the star graph and square lattice therefore illustrate the cases  
437 where this method is expected to perform least well. Testing Zachary's karate club [41] illustrates how this  
438 method might perform on a real world network. On this graph we find that Method 4 provides a reasonable  
439 approximation to the fixation probabilities (Table 2).

440 We also observed, as shown in Tables 1 and 2, that Method 4 performs most accurately when initiated on  
441 a node with average to high degree. In addition to approximating the fixation probability, Method 4 can be  
442 used to approximate the dynamics across the whole time series, and in particular provides a very accurate  
443 approximation to the initial dynamics for all graphs tested (see Figure 2 for results on two 20 node graphs  
444 as an illustration). This accuracy holds even for the large star graphs when initiated on the leaf node, for  
445 which the final approximation was close to 1.

#### 446 4.2. The Hawk-Dove game with the contact conditioning model

447 So far, we have considered the constant fitness case. Here we briefly consider the effectiveness of Method  
448 4 when applied to the Hawk-Dove game under the dynamics of the invasion process. Method 2 relies on  
449 finding a suitable scaling factor, whilst Methods 1 and 3 were both observed in Section 4.1 to yield non  
450 informative results on the type of graphs we test here and so we do not investigate these methods in this  
451 context.

452 The Hawk-Dove game [24, 23] represents a simple model of how animals compete over food, territory and  
453 other resources. Animals interact over a resource with either an aggressive or non-aggressive strategy, which

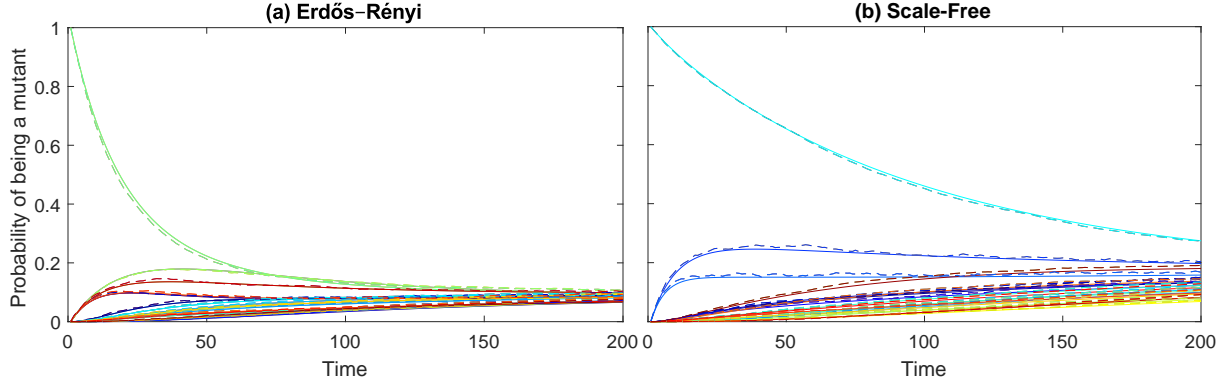


**Figure 2:** Comparison of the early dynamics of the marginal probabilities for each node on the graph being a mutant  $A$  plotted against time as given by Method 4 (solid lines) versus stochastic simulation (dashed lines), when applied to the invasion process on (a) an Erdős-Rényi random graph with 20 nodes and average degree of 4 and (b) a scale-free graph with 20 nodes and average degree 4, both initiated with a single  $A$  individual in a chosen node. Each line represents the marginal probability of a certain node in the graph being occupied by an  $A$  individual, the corresponding colours between the solid lines and dashed lines represent the same node on the graphs. The discrete-time stochastic process was simulated 10,000 times from the same initial condition, from which we obtained the probability for each node being a mutant at a given time as the proportion of simulations for which that node is a mutant. Method 4 was numerically integrated to approximate the probability of each node being a mutant at a given time. We use a dashed line with interpolation between integer time points for the discrete-time system to enable easier comparison of the dynamics. The game considered is the constant fitness case where the  $A$  individuals have fitness 1.2 and the  $B$  individuals have fitness 1.

454 we call the Hawk and Dove strategies, respectively. We let the resource yield a payoff  $V$  which both players  
 455 try to obtain. When two Hawks interact, they fight over the resource with one taking the payoff  $V$ , and the  
 456 other accruing a cost  $C$  from the fight, and therefore the average payoff received by a Hawk interacting with  
 457 a Hawk is  $(V - C)/2$ . When a Hawk meets a Dove, the Dove retreats without a fight receiving a payoff 0,  
 458 allowing the Hawk to take the whole resource, receiving payoff  $V$ . If two Doves meet, they either share the  
 459 resource, or each takes the whole reward without a fight with probability  $1/2$ , so that the average payoff  
 460 received by a Dove from this interaction is  $V/2$ . Therefore, in this game the payoff matrix is given by

$$\begin{matrix} & H & D \\ H & \left( \begin{matrix} (V - C)/2 & V \end{matrix} \right) \\ D & \left( \begin{matrix} 0 & V/2 \end{matrix} \right) \end{matrix}$$

461 Figure 3 illustrates results from this game on a scale-free graph, an Erdős-Rényi random graph, a  $k$ -regular  
 462 random graph and a square lattice. We consider two cases; firstly where the fight cost is low using parameters  
 463  $f_{back} = 2$ ,  $w = 1$ ,  $V = 1$  and  $C = 1.5$ , and secondly where the fight cost is high using parameters  $f_{back} = 2$ ,  
 464  $w = 1$ ,  $V = 1$  and  $C = 4$ . In each case we compare the results of Method 4 to stochastic simulation, initiated  
 465 with a population consisting of half Hawks and half Doves to minimise the chance of early extinction events.  
 466 We observe that when the cost is low the approximation is reasonable, with all 3 random graphs providing a  
 467 good approximation, and some accuracy lost on the square lattice. However, as we increase the cost,  $C$ , we  
 468 observe that the approximation does not perform well. This is because the contact conditioning assumption  
 469 seems to amplify the strength of the Hawk strategy, with the rate at which an individual becomes a Hawk  
 470 under this assumption being greater than it will be in the exact case.

## 471 5. Discussion

472 Evolutionary graph theory [20] was introduced as a way of adding spatial structure to the stochastic  
 473 evolutionary dynamics considered by Moran [25]. Analytic results on these stochastic dynamics focused

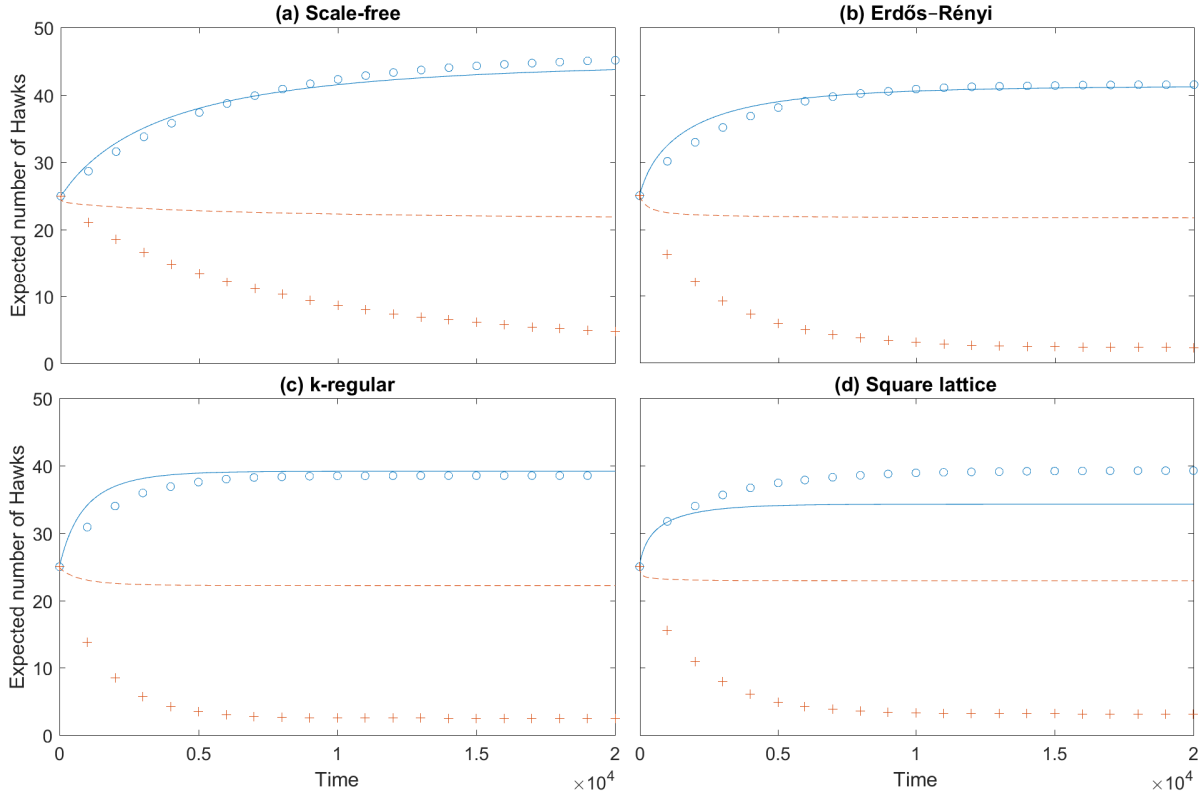


**Figure 3:** Comparison of the expected number of individuals playing the Hawk strategy in a Hawk-Dove game plotted against time as given by Method 4 versus stochastic simulation, when played on (a) a scale-free graph (b) an Erdős-Rényi graph (c) a  $k$ -regular random graph and (d) a 7 by 7 square lattice. Except for the square lattice, each graph has 50 nodes and an average degree of approximately 4. The solid lines represent the solution of Method 4 and the circles represent stochastic simulations of the discrete-time system, evaluated every 1000 time steps, in the case where  $C = 1.5$ . The dashed lines represent the solution of Method 4 and the crosses represent stochastic simulations of the discrete-time system, evaluated every 1000 time steps, in the case where  $C = 4$ . To generate the stochastic simulation results the discrete-time stochastic process was simulated 10,000 times from the same well mixed initial condition until fixation was reached. By taking the average number of Hawks at each time step we determined the expected number of Hawks at a given time. Method 4 is numerically integrated to give the probability of each node being a Hawk at a given time, from which we obtained the expected number of Hawks by summing over all nodes.

474 on idealised cases of simple graphs [2, 5]. In order to study arbitrary graphs, methods usually follow  
475 certain restrictions, such as focusing on the evolutionary process under weak selection or infinitely large  
476 populations [1, 28, 43]. Alternatively, individual-based stochastic simulations give very accurate results but  
477 are limited by computational time [3, 21].

478 The focus of this work has been the attempt to develop a general method that can approximate the  
479 stochastic dynamics on a wide range of graphs by adapting methods from statistical physics and epidemiology.  
480 In doing this, we have provided a derivation of existing (homogenised) pair-approximation models from the  
481 master equation [8, 10, 26, 30, 37] (Section 3.1). Additionally, we also derived an individual-level model  
482 which has the neutral drift model [32] as a special case (Section 3.2).

483 We start with a representation of the stochastic evolutionary process using a master equation [11],  
484 from which we develop exact equations describing individual node probabilities. We then apply ideas for  
485 approximating the master equation based around developing hierarchies of moment equations. Such methods  
486 were originally developed in physics [4, 16] and later used in epidemiology and ecology [10, 13, 29, 34, 35].  
487 The key idea behind these techniques is to write deterministic differential equations to describe how the  
488 probabilities of the states of individuals and pairs change over time.

489 We find that a major difference between evolutionary graph theory and other areas in which these  
490 methods have been applied is that here, event probabilities depend on the states of all individuals in the  
491 population. As a result, we do not obtain a precise BBGKY-like hierarchy, which relies on neighbouring  
492 particle-particle interactions. Another difference is that in evolutionary dynamics, we have two absorbing  
493 states, which potentially leads to system-wide correlations that cannot be captured on a local level. It is  
494 worth noting that some alternative nearest-neighbour interaction evolutionary models, which may yield such  
495 a hierarchy directly, have also been considered [39]; however, in this paper we have restricted our attention  
496 to the classic evolutionary graph theory dynamics.

497 In spite of these differences, some progress could be made towards approximating evolutionary dynamics.  
498 The first step was to write down equations for the rate of change of the state probabilities for individual  
499 nodes (Theorem 2.1). This led to equations which required conditioning against the probability of the state  
500 of the entire system, and therefore required the development of methods to simplify this. Motivated by  
501 an objective of deriving homogenised pair-approximation models used in the literature, our first approach  
502 was to modify the replacement rate by removing the normalisation by the total fitness (Section 3.1). This  
503 has the effect of altering the speed at which events occur but does not alter the final fixation probability.  
504 The resulting system of equations describes individual and pair probabilities in terms of the probability of  
505 their entire neighbourhoods. This could provide a basis to accurately approximate the fixation probability  
506 by finding appropriate moment closures to express the neighbourhoods as functions of individual and pair  
507 probabilities. However, this is difficult to implement and the number of equations increases exponentially  
508 with the maximum degree of the graph, making it infeasible in general without further approximation. By  
509 making further assumptions about the graph such that all individuals and pairs of a given type are identical  
510 and interchangeable, we were able to derive the homogenised pair approximation models [8, 26], which have  
511 been shown to give interesting results for various evolutionary games.

512 To obtain an approximation which is numerically feasible in general, we first ignored any conditioning,  
513 similar to a model in [37] which uses this assumption to construct a population level approximation. The  
514 resulting model (Equation (11)) was found to work well for small graphs and contains the exact neutral  
515 drift model [32] as a special case. However, as population size increases, the predictions for the fixation  
516 probability of a single mutant individual were observed to tend to zero. By solving this system for the  
517 fixation probability on a complete graph, we obtained a scaling factor which enabled this model to give a  
518 reasonable prediction of fixation probability from a given initial condition with a single mutant individual  
519 on any graph. Due to the construction of this method, it will perform best on graphs which yield average  
520 fixation probability close to the Moran probability.

521 To generate a more accurate model and one which does not require an artificial scaling factor, we in-  
522 vestigated models with some level of conditioning (Section 3.3). Conditioning against a single node results  
523 in the same level of complexity as conditioning against pairs of nodes and so we elected to produce results  
524 for the latter. In this case, we conditioned against the pair of nodes directly involved in the replacement  
525 event. However, in order to use this model on large graphs, we require the use of moment closure approxi-  
526 mations. We found that the standard method used in other areas with different closures for open and closed  
527 triples [13, 33] was not effective here because while it provides very good results on simple structures, on

528 most graphs it predicts fixation probabilities of either zero or one. It seems likely that this is caused by  
529 neglecting important graph-wide correlations across open triples associated with the two absorbing states of  
530 the system.

531 By using the Kirkwood closure method for all triples, including open ones, we obtained a method which  
532 provides informative predictions on the majority of graphs tested. We investigated square lattices and star-  
533 type graphs, as these are two extreme population structures which we use as worst case scenarios. The lattice  
534 is extreme as moment closure methods do not perform well on such graphs. The star is extreme because  
535 this type of graph significantly amplifies fixation probability, which seems to amplify the accumulated error  
536 in the approximation methods. For all three types of random graph considered, and Zachary's karate club,  
537 this method provides a reasonable approximation to the fixation probability. When the degree of the initial  
538 mutant node is not low the approximation can be very accurate. However, if we initiate on a low degree  
539 node, the method performs less well, potentially due to such nodes amplifying the fixation probability in the  
540 invasion process, again leading to inaccuracies in the solution being amplified. Despite potential inaccuracies  
541 in the fixation probability approximation, we observe that this method is particularly accurate for the early-  
542 time behaviour of these systems for any graph, and therefore can give interesting insights into this behaviour.  
543 The method is computationally feasible for reasonably large  $N$ , however, the computational complexity scales  
544 with  $N^2$  rather than with  $N$  which is more typical for epidemic models. Nevertheless, this still represents a  
545 significant reduction over the master equation which scales with  $2^N$ .

546 The novelty of this work is the adaption of well-established techniques from other fields to the study of  
547 evolutionary dynamics at the level of individual nodes. The contribution is two-fold. Firstly we have obtained  
548 insight into existing models by deriving them from the master equation. Secondly, the advantage of looking  
549 at node-level quantities rather than a homogenised model is that we gain the ability to compare dynamics  
550 from different initial conditions on the same graph, which is not present in many other approximation  
551 methods. Furthermore, the initial dynamics of Method 4 are very accurate (Figure 2), allowing us to see  
552 how the probability of each node being a mutant flows through the population. Although we chose to work  
553 in continuous time here and examples study the invasion process, similar methods could be followed directly  
554 in discrete-time and the methods are applicable to any Markovian update rule.

## 555 Acknowledgements

556 We would like to thank two anonymous reviewers for their valuable comments and suggestions which have  
557 contributed to strengthening the manuscript. CO and KS acknowledge support from the EPSRC Liverpool  
558 Centre for Mathematics in Healthcare (EP/N014499/1). CH and KS acknowledge support from EPSRC  
559 grant (EP/K503538/1). MB was supported by funding from the European Union's Horizon 2020 research  
560 and innovation programme under the Marie Skłodowska-Curie grant agreement No 690817.

- 561 [1] B. Allen, G. Lippner, Y. Chen, B. Fotouhi, N. Momeni, S. Yau, and M. A. Nowak. Evolutionary  
562 dynamics on any population structure. *Nature*, 544(7649):227–230, 2017.
- 563 [2] T. Antal, S. Redner, and V. Sood. Evolutionary dynamics on degree-heterogeneous graphs. *Physical  
564 Review Letters*, 96(18), 2006.
- 565 [3] V. C. Barbosa, R. Donangelo, and S. R. Souza. Early appraisal of the fixation probability in directed  
566 networks. *Physical Review E - Statistical, Nonlinear, and Soft Matter Physics*, 82(4), 2010.
- 567 [4] M. Born and H. S. Green. A general kinetic theory of liquids. i. the molecular distribution func-  
568 tions. *Proceedings of the Royal Society of London A: Mathematical, Physical and Engineering Sciences*,  
569 188(1012):10–18, 1946.
- 570 [5] M. Broom, C. Hadjichrysanthou, and J. Rychtář. Evolutionary games on graphs and the speed of the  
571 evolutionary process. *Proceedings of the Royal Society A: Mathematical, Physical and Engineering  
572 Sciences*, 466(2117):1327–1346, 2010.
- 573 [6] M. Broom and J. Rychtář. An analysis of the fixation probability of a mutant on special classes of non-  
574 directed graphs. *Proceedings of the Royal Society A: Mathematical, Physical and Engineering Sciences*,  
575 464(2098):2609–2627, 2008.

- 576 [7] P. Erdős and A. Rényi. On the evolution of random graphs. Publication of the Mathematical Institute  
577 of the Hungarian Academy of Sciences, 5(1):17–60, 1960.
- 578 [8] C. Hadjichrysanthou, M. Broom, and I. Z. Kiss. Approximating evolutionary dynamics on networks  
579 using a neighbourhood configuration model. *Journal of Theoretical Biology*, 312:13–21, 2012.
- 580 [9] C. Hadjichrysanthou, M. Broom, and J. Rychtář. Evolutionary games on star graphs under various  
581 updating rules. *Dynamic Games and Applications*, 1(3):386–407, 2011.
- 582 [10] C. Hauert and G. Szabó. Game theory and physics. *American Journal of Physics*, 73(5):405–414, 2005.
- 583 [11] L. Hindersin, M. Möller, A. Traulsen, and B. Bauer. Exact numerical calculation of fixation probability  
584 and time on graphs. *BioSystems*, 150:87–91, 2016.
- 585 [12] L. Hindersin and A. Traulsen. Most undirected random graphs are amplifiers of selection for birth-death  
586 dynamics, but suppressors of selection for death-birth dynamics. *PLoS Computational Biology*, 11(11),  
587 2015.
- 588 [13] M. J. Keeling. The effects of local spatial structure on epidemiological invasions. *Proceedings of the  
589 Royal Society B: Biological Sciences*, 266(1421):859–867, 1999.
- 590 [14] M. J. Keeling and K. T. D. Eames. Networks and epidemic models. *Journal of the Royal Society  
591 Interface*, 2(4):295–307, 2005.
- 592 [15] J. G. Kirkwood. Statistical mechanics of fluid mixtures. *The Journal of Chemical Physics*, 3(5):300–313,  
593 1935.
- 594 [16] J. G. Kirkwood. The statistical mechanical theory of transport processes ii. transport in gases. *The  
595 Journal of Chemical Physics*, 15(1):72–76, 1947.
- 596 [17] J. G. Kirkwood and E. M. Boggs. The radial distribution function in liquids. *The Journal of Chemical  
597 Physics*, 10(6):394–402, 1942.
- 598 [18] I. Z. Kiss, J. C. Miller, and P. L. Simon. *Mathematics of epidemics on networks*. Cham: Springer, 2017.
- 599 [19] I. Z. Kiss, C. G. Morris, F. Sélley, P. L. Simon, and R. R. Wilkinson. Exact deterministic representation  
600 of markovian s i r epidemics on networks with and without loops. *Journal of mathematical biology*,  
601 70(3):437–464, 2015.
- 602 [20] E. Lieberman, C. Hauert, and M. A. Nowak. Evolutionary dynamics on graphs. *Nature*, 433(7023):312–  
603 316, 2005.
- 604 [21] W. Maciejewski, F. Fu, and C. Hauert. Evolutionary game dynamics in populations with heterogenous  
605 structures. *PLOS Computational Biology*, 10:1–16, 04 2014.
- 606 [22] N. Masuda. Directionality of contact networks suppresses selection pressure in evolutionary dynamics.  
607 *Journal of Theoretical Biology*, 258(2):323–334, 2009.
- 608 [23] J. Maynard Smith. *Evolution and the Theory of Games*. Cambridge university press, 1982.
- 609 [24] J. Maynard Smith and G. R. Price. The logic of animal conflict. *Nature*, 246(5427):15, 1973.
- 610 [25] P. A. P. Moran. Random processes in genetics. *Mathematical Proceedings of the Cambridge Philosophical  
611 Society*, 54(1):60–71, 1958.
- 612 [26] S. Morita. Extended pair approximation of evolutionary game on complex networks. *Progress of  
613 Theoretical Physics*, 119(1):29–38, 2008.
- 614 [27] M. A. Nowak, C. E. Tarnita, and T. Antal. Evolutionary dynamics in structured populations. *Philosophical  
615 Transactions of the Royal Society of London B: Biological Sciences*, 365(1537):19–30, 2010.

- 616 [28] H. Ohtsuki, C. Hauert, E. Lieberman, and M. A. Nowak. A simple rule for the evolution of cooperation  
617 on graphs and social networks. *Nature*, 441(7092):502–505, 2006.
- 618 [29] L. Pellis, T. House, and M. J. Keeling. Exact and approximate moment closures for non-markovian  
619 network epidemics. *Journal of Theoretical Biology*, 382:160–177, 2015.
- 620 [30] J. Pena, H. Volken, E. Pestelacci, and M. Tomassini. Conformity hinders the evolution of cooperation  
621 on scale-free networks. *Physical Review E*, 80(1):016110, 2009.
- 622 [31] T. Rogers. Maximum-entropy moment-closure for stochastic systems on networks. *Journal of Statistical  
623 Mechanics: Theory and Experiment*, 2011(05):P05007, 2011.
- 624 [32] P. Shakarian, P. Roos, and G. Moores. A novel analytical method for evolutionary graph theory prob-  
625 lems. *BioSystems*, 111(2):136–144, 2013.
- 626 [33] K. J. Sharkey. Deterministic epidemiological models at the individual level. *Journal of Mathematical  
627 Biology*, 57(3):311–331, 2008.
- 628 [34] K. J. Sharkey, I. Z. Kiss, R. R. Wilkinson, and P. L. Simon. Exact equations for SIR epidemics on tree  
629 graphs. *Bulletin of Mathematical Biology*, 77(4):614–645, 2015.
- 630 [35] K. J. Sharkey and R. R. Wilkinson. Complete hierarchies of SIR models on arbitrary networks with  
631 exact and approximate moment closure. *Mathematical Biosciences*, 264(1):74–85, 2015.
- 632 [36] A. Singer. Maximum entropy formulation of the kirkwood superposition approximation. *The Journal  
633 of Chemical Physics*, 121(8):3657–3666, 2004.
- 634 [37] G. Szabó and G. Fath. Evolutionary games on graphs. *Physics Reports*, 446(4-6):97–216, 2007.
- 635 [38] C. Taylor, D. Fudenberg, A. Sasaki, and M. A. Nowak. Evolutionary game dynamics in finite popula-  
636 tions. *Bulletin of Mathematical Biology*, 66(6):1621–1644, 2004.
- 637 [39] A. Traulsen, J. C. Claussen, and C. Hauert. Coevolutionary dynamics: From finite to infinite popula-  
638 tions. *Physical Review Letters*, 95:238701, 2005.
- 639 [40] A. Traulsen and C. Hauert. *Stochastic Evolutionary Game Dynamics*, volume 2 of *Reviews of Nonlinear  
640 Dynamics and Complexity*, pages 25–61. 2010.
- 641 [41] W. W. Zachary. An information flow model for conflict and fission in small groups. *Journal of Anthro-  
642 pological Research*, 33(4):452–473, 1977.
- 643 [42] P. Zhang, P. Nie, D. Hu, and F. Zou. The analysis of bi-level evolutionary graphs. *BioSystems*,  
644 90(3):897–902, 2007.
- 645 [43] W. Zhong, J. Liu, and L. Zhang. Evolutionary dynamics of continuous strategy games on graphs and  
646 social networks under weak selection. *BioSystems*, 111(2):102–110, 2013.

## 647 Appendices

### 648 Appendix A Proof of Theorem 2.1

649 *Proof.* By total probability rules we have that

$$\frac{dP(A_{\{i\}}^t)}{dt} = \frac{d \left[ \sum_{X_{V \setminus \{i\}}} P(A_{\{i\}}^t X_{V \setminus \{i\}}^t) \right]}{dt} = \sum_{X_{V \setminus \{i\}}} \frac{dP(A_{\{i\}}^t X_{V \setminus \{i\}}^t)}{dt}, \quad (\text{A.1})$$

650 where  $X_{V \setminus \{i\}}$  is the state of the nodes in the system not including  $i$ .

651 Consider a set state  $X_{V \setminus \{i\}}$  of the remaining nodes. The rate of change in the full system state probability  
 652  $P(A_{\{i\}}^t X_{V \setminus \{i\}}^t)$  is given by

$$\begin{aligned} \frac{dP(A_{\{i\}}^t X_{V \setminus \{i\}}^t)}{dt} &= \sum_{Y_{V \setminus \{i\}}} P(A_{\{i\}}^t Y_{V \setminus \{i\}}^t) \chi(A_{\{i\}}^t Y_{V \setminus \{i\}}^t \rightarrow A_{\{i\}}^t X_{V \setminus \{i\}}^t) \\ &\quad + P(B_{\{i\}}^t X_{V \setminus \{i\}}^t) \chi(B_{\{i\}}^t X_{V \setminus \{i\}}^t \rightarrow A_{\{i\}}^t X_{V \setminus \{i\}}^t) \\ &\quad - \sum_{Y_{V \setminus \{i\}}} P(A_{\{i\}}^t X_{V \setminus \{i\}}^t) \chi(A_{\{i\}}^t X_{V \setminus \{i\}}^t \rightarrow A_{\{i\}}^t Y_{V \setminus \{i\}}^t) \\ &\quad - P(A_{\{i\}}^t X_{V \setminus \{i\}}^t) \chi(A_{\{i\}}^t X_{V \setminus \{i\}}^t \rightarrow B_{\{i\}}^t X_{V \setminus \{i\}}^t), \end{aligned} \quad (\text{A.2})$$

653 where  $\chi(A_{\{i\}}^t X_{V \setminus \{i\}}^t \rightarrow B_{\{i\}}^t X_{V \setminus \{i\}}^t)$  is the rate at which the system moves from state  $A_{\{i\}}^t X_{V \setminus \{i\}}^t$  to state  
 654  $B_{\{i\}}^t X_{V \setminus \{i\}}^t$ .

655 Consider the terms which involve changing the state of the individual in node  $i$  in Equation (A.2), by  
 656 expanding the rate into the sum of separate event rates we obtain

$$P(B_{\{i\}}^t X_{V \setminus \{i\}}^t) \chi(B_{\{i\}}^t X_{V \setminus \{i\}}^t \rightarrow A_{\{i\}}^t X_{V \setminus \{i\}}^t) = P(B_{\{i\}}^t X_{V \setminus \{i\}}^t) \sum_{j=1}^N G_{ij} \chi(\Omega_{j \rightarrow i}^t | B_{\{i\}}^t X_{V \setminus \{i\}}^t) \mathbf{1}_{(A_{\{j\}}^t \in X_{V \setminus \{i\}}^t)},$$

657 and

$$P(A_{\{i\}}^t X_{V \setminus \{i\}}^t) \chi(A_{\{i\}}^t X_{V \setminus \{i\}}^t \rightarrow B_{\{i\}}^t X_{V \setminus \{i\}}^t) = P(A_{\{i\}}^t X_{V \setminus \{i\}}^t) \sum_{j=1}^N G_{ij} \chi(\Omega_{j \rightarrow i}^t | A_{\{i\}}^t X_{V \setminus \{i\}}^t) \mathbf{1}_{(B_{\{j\}}^t \in X_{V \setminus \{i\}}^t)},$$

658 where  $\mathbf{1}_{(B_{\{j\}}^t \in X_{V \setminus \{i\}}^t)}$  is an indicator function on the event  $B_{\{j\}}^t$  being part the event  $X_{V \setminus \{i\}}^t$ . That is, the  
 659 state of node  $j$  in the state  $X$  is type  $B$ . The  $\chi(\Omega_{j \rightarrow i}^t | A_{\{i\}}^t X_{V \setminus \{i\}}^t)$  term is the rate at which the individual  
 660 in node  $j$  replaces the individual in node  $i$ , given that the system is in state  $A_{\{i\}}^t X_{V \setminus \{i\}}^t$ , as defined in  
 661 Definition 2.1. Rearranging these and substituting into Equation (A.2) gives

$$\begin{aligned} \frac{dP(A_{\{i\}}^t X_{V \setminus \{i\}}^t)}{dt} &= \sum_{j=1}^N G_{ij} P(B_{\{i\}}^t X_{V \setminus \{i\}}^t) \chi(\Omega_{j \rightarrow i}^t | B_{\{i\}}^t X_{V \setminus \{i\}}^t) \mathbf{1}_{(A_{\{j\}}^t \in X_{V \setminus \{i\}}^t)} \\ &\quad - \sum_{j=1}^N G_{ij} P(A_{\{i\}}^t X_{V \setminus \{i\}}^t) \chi(\Omega_{j \rightarrow i}^t | A_{\{i\}}^t X_{V \setminus \{i\}}^t) \mathbf{1}_{(B_{\{j\}}^t \in X_{V \setminus \{i\}}^t)} \\ &\quad + \sum_{Y_{V \setminus \{i\}}} P(A_{\{i\}}^t Y_{V \setminus \{i\}}^t) \chi(A_{\{i\}}^t Y_{V \setminus \{i\}}^t \rightarrow A_{\{i\}}^t X_{V \setminus \{i\}}^t) \\ &\quad - \sum_{Y_{V \setminus \{i\}}} P(A_{\{i\}}^t X_{V \setminus \{i\}}^t) \chi(A_{\{i\}}^t X_{V \setminus \{i\}}^t \rightarrow A_{\{i\}}^t Y_{V \setminus \{i\}}^t) \end{aligned}$$

662 By substituting this into Equation (A.1) we obtain

$$\begin{aligned}
\frac{dP(A_{\{i\}}^t)}{dt} &= \sum_{X_{V \setminus \{i\}}} \sum_{j=1}^N G_{ij} P(B_{\{i\}}^t X_{V \setminus \{i\}}^t) \chi(\Omega_{j \rightarrow i}^t | B_{\{i\}}^t X_{V \setminus \{i\}}^t) \mathbf{1}_{(A_{\{j\}}^t \in X_{V \setminus \{i\}}^t)} \\
&\quad - \sum_{X_{V \setminus \{i\}}} \sum_{j=1}^N G_{ij} P(A_{\{i\}}^t X_{V \setminus \{i\}}^t) \chi(\Omega_{j \rightarrow i}^t | A_{\{i\}}^t X_{V \setminus \{i\}}^t) \mathbf{1}_{(B_{\{j\}}^t \in X_{V \setminus \{i\}}^t)} \\
&\quad + \sum_{X_{V \setminus \{i\}}} \sum_{Y_{V \setminus \{i\}}} P(A_{\{i\}}^t Y_{V \setminus \{i\}}^t) \chi(A_{\{i\}}^t Y_{V \setminus \{i\}}^t \rightarrow A_{\{i\}}^t X_{V \setminus \{i\}}^t) \\
&\quad - \sum_{X_{V \setminus \{i\}}} \sum_{Y_{V \setminus \{i\}}} P(A_{\{i\}}^t X_{V \setminus \{i\}}^t) \chi(A_{\{i\}}^t X_{V \setminus \{i\}}^t \rightarrow A_{\{i\}}^t Y_{V \setminus \{i\}}^t).
\end{aligned}$$

663 Clearly the last two sums cancel, so we can simplify this to

$$\begin{aligned}
\frac{dP(A_{\{i\}}^t)}{dt} &= \sum_{j=1}^N \sum_{X_{V \setminus \{i,j\}}} G_{ij} P(B_{\{i\}}^t A_{\{j\}}^t X_{V \setminus \{i,j\}}^t) \chi(\Omega_{j \rightarrow i}^t | B_{\{i\}}^t A_{\{j\}}^t X_{V \setminus \{i,j\}}^t) \\
&\quad - \sum_{j=1}^N \sum_{X_{V \setminus \{i,j\}}} G_{ij} P(A_{\{i\}}^t B_{\{j\}}^t X_{V \setminus \{i,j\}}^t) \chi(\Omega_{j \rightarrow i}^t | A_{\{i\}}^t B_{\{j\}}^t X_{V \setminus \{i,j\}}^t),
\end{aligned}$$

664 as required. □

## 665 Appendix B Derivation of the scaling factor (Equation 12)

666 *Proof.* Consider a system with rate of change given by

$$\frac{d\bar{P}(A_{\{i\}}^t)}{dt} = \sum_{j=1}^N G_{ij} \bar{P}(A_{\{j\}}^t) \chi(\Omega_{j \rightarrow i}^t) - \sum_{j=1}^N G_{ij} \bar{P}(A_{\{i\}}^t) \chi(\Omega_{j \rightarrow i}^t).$$

667 Since we are interested in the complete graph, we have that  $G_{ij} = 1$  for  $j \neq i$ , and  $G_{i,i} = 0$ . Let  $A_c$  denote  
668 the average probability that a node is of type  $A$  on the complete graph at time  $t$ . That is

$$A_c(t) = \frac{1}{N} \sum_{j=1}^N \bar{P}(A_{\{j\}}^t) = \frac{S}{N}.$$

669 Since we are considering constant fitness we have

$$\chi(\Omega_{j \rightarrow i}^t) = \frac{\bar{P}(A_{\{j\}}^t)(r-1) + 1}{\sum_{k=1}^N \bar{P}(A_{\{k\}}^t)(r-1) + 1} = \frac{\bar{P}(A_{\{j\}}^t)(r-1) + 1}{N + (r-1)S},$$

670 which gives us

$$\frac{dS}{dt} = \sum_{i=1}^N \frac{d\bar{P}(A_{\{i\}}^t)}{dt} = \frac{\sum_{i,j=1}^N (\bar{P}(A_{\{j\}}^t) - \bar{P}(A_{\{i\}}^t)) (\bar{P}(A_{\{j\}}^t)(r-1) + 1)}{N + (r-1)S}.$$

671 Writing  $G = \sum_{i,j=1}^N (\bar{P}(A_{\{j\}}^t) - \bar{P}(A_{\{i\}}^t)) \bar{P}(A_{\{j\}}^t)$ , and  $H = \sum_{i,j=1}^N (\bar{P}(A_{\{j\}}^t) - \bar{P}(A_{\{i\}}^t))$  we have

$$\frac{dS}{dt} = \frac{(r-1)G + H}{N + (r-1)S}.$$

672 Clearly  $H = 0$ , so we obtain

$$\frac{dS}{dt} = \frac{(r-1)G}{N + (r-1)S}.$$

673 Note that  $\sum_{i,j=1}^N (\bar{P}(A_{\{j\}}^t) - \bar{P}(A_{\{i\}}^t))^2 = \sum_{i,j=1}^N \bar{P}(A_{\{j\}}^t)^2 + \bar{P}(A_{\{i\}}^t)^2 - 2\bar{P}(A_{\{j\}}^t)\bar{P}(A_{\{i\}}^t) = 2G$ , so that

$$\frac{dG}{dt} = \frac{1}{2} \frac{d}{dt} \left( \sum_{i,j=1}^N (\bar{P}(A_{\{j\}}^t) - \bar{P}(A_{\{i\}}^t))^2 \right) = \sum_{i,j=1}^N (\bar{P}(A_{\{j\}}^t) - \bar{P}(A_{\{i\}}^t)) \frac{d(\bar{P}(A_{\{j\}}^t) - \bar{P}(A_{\{i\}}^t))}{dt}.$$

674 Considering the last term on the right hand side we have

$$\begin{aligned} \frac{d(\bar{P}(A_{\{i\}}^t) - \bar{P}(A_{\{j\}}^t))}{dt} &= \frac{1}{N + (r-1)S} \sum_{k=1}^N (\bar{P}(A_{\{k\}}^t)(\bar{P}(A_{\{k\}}^t) - \bar{P}(A_{\{i\}}^t)) + \bar{P}(A_{\{k\}}^t)(\bar{P}(A_{\{j\}}^t) - \bar{P}(A_{\{k\}}^t)))(r-1) \\ &\quad + (\bar{P}(A_{\{k\}}^t) - \bar{P}(A_{\{i\}}^t)) + (\bar{P}(A_{\{j\}}^t) - \bar{P}(A_{\{k\}}^t)) \\ &= \frac{1}{N + (r-1)S} \sum_{k=1}^N \bar{P}(A_{\{k\}}^t)(\bar{P}(A_{\{j\}}^t) - \bar{P}(A_{\{i\}}^t))(r-1) + (\bar{P}(A_{\{j\}}^t) - \bar{P}(A_{\{i\}}^t)) \\ &= \frac{(\bar{P}(A_{\{j\}}^t) - \bar{P}(A_{\{i\}}^t))((r-1)S + N)}{N + (r-1)S} \\ &= -(\bar{P}(A_{\{i\}}^t) - \bar{P}(A_{\{j\}}^t)). \end{aligned}$$

675 Thus,

$$\frac{dG}{dt} = \sum_{i,j=1}^N (\bar{P}(A_{\{j\}}^t) - \bar{P}(A_{\{i\}}^t))^2 = -2G \implies G = Ae^{-2t} = (N-m)me^{-2t},$$

676 since  $G(0) = (N-m)m$ . Therefore we have

$$\frac{dS}{dt} = \frac{(r-1)(N-m)me^{-2t}}{N + (r-1)S}$$

$$\implies NS + \frac{r-1}{2}S^2 = -\frac{1}{2}(r-1)(N-m)me^{-2t} + C.$$

677 At  $t = 0$  we have  $S = \sum \bar{P}(A_{\{j\}}^t) = m$ , which gives

$$C = Nm + \left(\frac{r-1}{2}\right)Nm = Nm\left(\frac{r+1}{2}\right),$$

678 and so we can solve to obtain

$$S = \frac{(-N \pm \sqrt{N^2 + 4\frac{r-1}{2}(Nm\frac{r+1}{2} - (N-m)m\frac{r-1}{2}e^{-2t})})}{r-1}.$$

679 Only the positive root makes sense, so we obtain

$$A_c = \frac{1}{r-1} \left( -1 + \sqrt{1 + \frac{m(r^2-1)}{N} - (r-1)^2 \frac{(N-m)m}{N^2} e^{-2t}} \right).$$

680 Thus, we have  $\lim_{t \rightarrow \infty} A_c(t) = \frac{1}{r-1} \left( -1 + \sqrt{1 + \frac{m(r^2-1)}{N}} \right)$ . □